Prepared for submission to JHEP

SLAC–P–24002

arXiv:2411.01571v2 [hep-th] 11 Jan 2025

A Two-Loop Four-Point Form Factor at Function Level

Lance J. Dixon[1] **and Shuo Xin**[1]

[1] *SLAC National Accelerator Laboratory, Stanford University, Stanford, CA 94309, USA*

E-mail: lance@slac.stanford.edu, xinshuo@stanford.edu

Abstract: Recently, the maximally-helicity-violating four-point form factor for the chiral stress-energy tensor in planar $\mathcal{N} = 4$ super Yang-Mills was computed to three loops at the level of the symbol associated with multiple polylogarithms. It exhibits *antipodal self-duality*, or invariance under the combined action of a kinematic map and reversing the ordering of letters in the symbol. Here we lift the two-loop form factor from symbol level to function level. We provide an iterated representation of the function's derivatives (coproducts). In order to do so, we find a three-parameter limit of the five-parameter phase space where the symbol's letters are all rational. We also use function-level information about dihedral symmetries and the soft, collinear, and factorization limits, as well as limits governed by the form-factor operator product expansion (FFOPE). We provide plots of the remainder function on several kinematic slices, and show that the result is compatible with the FFOPE data. We further verify that antipodal self-duality is valid at two loops beyond the level of the symbol.

Contents

1 Introduction **1**

2 Four-particle form factor and generalized polylogarithms **4**
- 2.1 BDS-like normalized form factors 4
- 2.2 Polylogarithms and (antipodable-)symbol alphabet 6

3 Integrating the symbol up to functions **8**
- 3.1 Function space 9
- 3.2 Boundary kinematics 11
  - 3.2.1 Rational surface and soft/collinear factorization 11
  - 3.2.2 FFOPE limit: Near multi-collinear factorization 15
  - 3.2.3 2D kinematics 17
- 3.3 Dihedral symmetry constraints 18

4 Remainder function in the bulk **18**
- 4.1 Slices through the rational surface 19
- 4.2 Antipodal duality beyond the symbol 19

5 Conclusion **23**

A Remainder function near the OPE limit **25**

B Remainder function in 2D kinematics **30**

C Remainder function near $u_1, u_2, u_3 \to 0$ **31**

1 Introduction

Perturbative calculations of scattering amplitudes and form factors in planar $\mathcal{N} = 4$ super-Yang-Mills (SYM) theory have seen tremendous progress in recent years. Among many recent developments, bootstrap methods have proven to be particularly effective in pushing the results to both high multiplicity and high loop orders [1–16]. A critical ingredient for such methods is sufficient boundary-value data, which can be supplied by the flux-tube representation or pentagon operator-product expansion (OPE) [17–22]. This representation has recently been extended to form factors of protected operators (FFOPE) [23–26]. Another source of boundary-value data for amplitudes is multi-Regge kinematics [27, 28], which has been understood to all subleading logarithms for six-point scattering [29] and beyond [30].

Three-point form factors can also exhibit factorized Regge behavior [16]. On the other hand, the multi-Regge behavior of higher-point form factors is still ripe for exploration.

In the planar limit of a large number of colors, $\mathcal{N} = 4$ SYM exhibits remarkable properties, such as the amplitude/Wilson loop duality [31–43] and dual conformal invariance [31, 44–47]. Such discoveries are often fueled by perturbative results at high multiplicity and loop orders.

Recently, a novel antipodal duality has emerged from bootstrapped amplitudes and form factors. The six-gluon maximally-helicity-violating (MHV) scattering amplitude had been bootstrapped to seven loops [12]. The three-point form factor for the chiral stress-tensor operator (or equivalently $\mathrm{tr}\phi^2$) was then bootstrapped to eight loops [13, 14]. These two quantities turn out to be related by *antipodal duality* [48]: the combined action of a kinematic map and reversing the order of letters in all terms in the symbol. The kinematic map maps the two-parameter phase space for the form factor into a parity-preserving slice of the three-parameter phase space for the six-point amplitude. This duality can be checked to hold beyond the symbol, at least modulo $i\pi$ terms which are not specified by the antipodal action on the Hopf algebra for multiple polylogarithms [48].

More recently, the *four*-point MHV form factor for the same $\mathrm{tr}\phi^2$ operator has been shown to exhibit antipodal *self*-duality on a four-dimensional (parity-preserving) slice of its five-dimensional phase space [49]. This self-duality encompasses the previous duality, in the sense that the kinematic map in the four-point form factor relates two different limits, one which produces the three-point form factor, and the other produces the six-gluon scattering amplitude (because it is also a triple-collinear splitting amplitude). On the other hand, there is no fundamental understanding of why antipodal *self*-duality should exist, nor has it been verified yet beyond the symbol level.

Indeed, many high-order and high-multiplicity results to date are limited to the symbol level, which leaves much beyond-the-symbol information and numerical behavior unexplored. Efforts have been made to recover the full function level information for six-point amplitudes [3–5, 7, 8, 12] and, more recently, seven-point scattering amplitudes [50]. In fact, antipodal duality has been exploited to obtain the MHV six-point amplitude at eight loops at function level [15].

The three-point $\mathrm{tr}\phi^2$ form factor [13, 14] has also been fixed at function level through eight loops. However, beyond one loop, the knowledge of the four-point MHV $\mathrm{tr}\phi^2$ form factor was, until very recently [61], limited to symbol level [49] and a special limit in which the operator has a light-like momentum [51].[1]

One difficulty in lifting the four-point MHV $\mathrm{tr}\phi^2$ form factor to a function is the large and intricate symbol alphabet: The alphabet for the three-point $\mathrm{tr}\phi^2$ form factor has only 6 letters, while that for the six-point and seven-point amplitude have 9 and 42 letters, respectively [54, 55]. The symbol alphabet for the four-point MHV $\mathrm{tr}\phi^2$ form factor at two (three) loops has 34 (88) letters [49]. While seven-point scattering amplitudes have been successfully lifted from

[1] The four-point $\mathrm{tr}\phi^3$ form factor, on the other hand, involves simpler Feynman integrals than $\mathrm{tr}\phi^2$; it has been computed at two loops using a bootstrap based on master integrals [52]. (The three-point $\mathrm{tr}\phi^3$ form factor was very recently computed through six loops [16, 53].)

symbol-level to function level [50], the symbol alphabet in that case has only 42 letters, and is considerably easier to rationalize by a suitable choice of kinematical variables, compared with the 34 (88) letter alphabet for the four-point MHV $\mathrm{tr}\phi^2$ form factor.

Lifting the symbol of the four-point MHV $\mathrm{tr}\phi^2$ form factor to a full function would bring several new pieces of information. The numerical values, which are unavailable from only the symbol, could (if evaluated to high enough loop order) probe the radius of convergence of perturbation theory [4, 7, 12]. It might also be possible to interpolate or extrapolate to strong coupling where a minimal surface formulation is available [31, 41, 56]. In the case of amplitudes, such interpolation is relatively simple at special kinematic points called origins [57, 58], but it is also possible in the OPE limit [17, 23]. Antipodal self-duality can be analyzed beyond symbol level. Various Minkowski factorization limits can also be studied, such as multi-Regge kinematics, the self-crossing (or pseudo-double-parton scattering) limit [12, 59, 60], and the light-like limit [51].

In this paper we uplift the two-loop four-point MHV form factor for $\mathrm{tr}\phi^2$ from its symbol to a full function of the kinematics. We do so by specifying the iterated coproducts of the function (essentially its derivatives) in a space of polylogarithmic functions with weight up to three, as well as specifying their boundary values at a particular point in the phase space. We make special use of a three-parameter subspace of the five-parameter phase space where all the symbol letters rationalize, which we call the *rational surface*. We write the form factor remainder explicitly in terms of multiple polylogarithms on this surface, and use that representation to move from region to region on the surface.

We fix beyond-the-symbol constants (which are zeta values) using invariance under the dihedral symmetry group D_4, and using the universal factorization behavior in kinematic limits, including where a particle becomes soft, or two or three particles become collinear. We also match the near-collinear limit to data from the FFOPE [23–26].

Very recently, the four-point MHV $\mathrm{tr}\phi^2$ form factor has also been computed at two loops [61] at function level, by using unitarity cut methods to obtain the loop integrands in D spacetime dimensions. Integration-by-parts reduction was then used to write the result in terms of the basis of two-loop, non-planar five-point master integrals with one external mass provided in ref. [62]. These master integrals are provided in a $2 \to 3$ scattering configuration. Ref. [61] also used AMFlow [63] to compute a couple of numerical values in (pseudo-)Euclidean or $1 \to 4$ decay kinematics. As we focus mainly on the Euclidean region in our paper, and provide more analytic results, our results are complementary to those of ref. [61].

This paper is organized as follows. In Sec. 2 we introduce our notation and review basic properties of form factors and multiple polylogarithms. In Sec. 3 we define the space of functions used to describe the four-point MHV $\mathrm{tr}\phi^2$ form factor. We also describe the three-parameter rational surface kinematics. We then fix all the beyond-the-symbol constants by utilizing the available information. We provide the result for the remainder function in the bulk in Sec. 4. We conclude in Sec. 5 with a discussion of future research directions enabled by this work.

Many of the explicit results of this paper are rather lengthy, so they are included as computer-readable ancillary files: `AntipodalAlphabet.m` specifies the symbol alphabet we work with. `R42funcCoTable.m` gives the iterated coproducts of the function in terms of a set of independent lower-weight functions we call P functions. `R42_rational.m` is the representation of the remainder function on the rational surface in terms of multiple polylogarithms. `Prat.m` provides the same representation for the P functions. `PTT2to0_xy.m` provides the P functions in the OPE limit (defined in Sec. 3). `R42_OPE.txt` provides the set of coefficient functions describing the remainder function in the OPE limit (see Appendix A).

2 Four-particle form factor and generalized polylogarithms

2.1 BDS-like normalized form factors

In this paper, we study the MHV form factor for the chiral stress energy tensor in planar $\mathcal{N} = 4$ SYM. One representative for this BPS-protected operator super-multiplet is $\mathrm{tr}\phi^2$, where ϕ^2 is some traceless (non-Konishi) scalar bilinear, and the trace "tr" is over the large-N_c $SU(N_c)$ gauge group. One component of the super four-point form factor is the matrix element of $\mathrm{tr}\phi^2$ with two massless scalars and two same-helicity gluons:

$$\mathcal{F}_4^{\mathrm{MHV}} = \langle \mathrm{tr}\phi^2(q)\, \phi(p_1)\phi(p_2)g^+(p_3)g^+(p_4)\rangle \,. \tag{2.1}$$

This form factor was first computed at one loop [37], and then at two loops at symbol level [49]. Our task is to provide a function-level description.

The operator momentum q^μ is the sum of the momenta of the four massless particles,

$$q^\mu = \sum_{i=1}^{4} p_i^\mu \,, \tag{2.2}$$

where $p_i^2 = 0$. The form factor depends on the external momenta p_i through the dimensionless ratios,

$$u_i \equiv \frac{(p_i + p_{i+1})^2}{q^2} \,, \qquad v_i \equiv \frac{(p_i + p_{i+1} + p_{i+2})^2}{q^2} \,, \tag{2.3}$$

where $i = 1, 2, 3, 4$ and all indices are mod 4. These eight dimensionless ratios are constrained by three relations from the masslessness of the p_i and momentum conservation:

$$-u_1 + u_3 + v_4 + v_1 = 1 \,, \tag{2.4}$$

$$-u_2 + u_4 + v_1 + v_2 = 1 \,, \tag{2.5}$$

$$-u_3 + u_1 + v_2 + v_3 = 1 \,. \tag{2.6}$$

There is a D_4 dihedral symmetry, which is generated by two transformations,

$$\textbf{cycle } (\mathcal{C}): \quad p_i \to p_{i+1} \quad \Rightarrow \quad u_i \to u_{i+1} \,, \quad v_i \to v_{i+1} \,, \tag{2.7}$$

$$\textbf{flip } (\mathcal{F}): \quad p_2 \leftrightarrow p_4 \quad \Rightarrow \quad u_1 \leftrightarrow u_4 \,, \quad u_2 \leftrightarrow u_3 \,, \quad v_1 \leftrightarrow v_3 \,. \tag{2.8}$$

Following ref. [49], we normalize the MHV form factor (2.1) by a BDS-like form factor which only depends on two-particle Lorentz invariants. We define the function $\mathcal{E}_4$ by

$$\mathcal{F}_4^{\text{MHV}} = \mathcal{F}_4^{\text{MHV,tree}} \times \exp\left[-\frac{\Gamma_{\text{cusp}}(g^2)}{4\,\epsilon^2}\sum_{i=1}^{4}\left(\frac{\mu^2}{-s_{i,i+1}}\right)^{\epsilon}\right] \times \mathcal{E}_4\,, \tag{2.9}$$

where the 't Hooft coupling is $g^2 = N_c g_{\text{YM}}^2/(16\pi^2)$ and the cusp anomalous dimension in planar $\mathcal{N}=4$ SYM is [64]

$$\Gamma_{\text{cusp}}(g^2) = 4g^2 - 8\zeta_2 g^4 + 88\zeta_4 g^6 - 4\left[219\zeta_6 + 8(\zeta_3)^2\right] g^8 + \dots\,. \tag{2.10}$$

We define the *remainder function* $\mathcal{R}_4$ by dividing by the exponential of the full one-loop form factor (and taking the logarithm). It is related to $\mathcal{E}_4$ by

$$\mathcal{E}_4 = \exp\left[\frac{\Gamma_{\text{cusp}}}{4}\mathcal{E}_4^{(1)} + \mathcal{R}_4\right], \tag{2.11}$$

where the one-loop function $\mathcal{E}_4^{(1)}$ is the finite part of the one-loop amplitude, and is given by

$$\mathcal{E}_4^{(1)} = -2\,\text{Li}_2\big(1-v_1\big) - \text{Li}_2\Big(1-\frac{u_2}{v_1 v_2}\Big) - \ln u_1 \ln u_2 + \ln v_1 \ln\Big(\frac{u_1 u_2}{v_1 v_2}\Big) + \zeta_2 \;+\; \text{cyclic}. \tag{2.12}$$

Here "+ cyclic" means to add the three images under the cyclic transformation $\mathcal{C}$ in eq. (2.7).

The form factor also has a representation in terms of a light-like polygonal Wilson loop, which only closes in a space that is periodic by q, in order to account for the operator momentum [37]. In order to define a finite periodic polygonal Wilson loop, one can normalize by suitable lower-point quantities, resulting in a "framed" Wilson loop $\mathcal{W}_4$ [23–25]. The framed Wilson loop is related to the form-factor remainder function by

$$\mathcal{W}_4 = \exp\left[\frac{\Gamma_{\text{cusp}}}{4}\mathcal{W}_4^{(1)} + \mathcal{R}_4\right], \tag{2.13}$$

where

$$\begin{aligned}\mathcal{W}_4^{(1)} \;=\; & \mathcal{E}_4^{(1)} + \ln^2(v_1 v_4 - u_1) + 2\ln^2(1-v_4) + 2\ln^2 v_4 \\ & - \ln(v_1 v_4 - u_1)[2\ln v_4 - 2\ln(1-v_4) + \ln u_1 + \ln u_2 + \ln u_3 - \ln u_4] \\ & - 2\ln(1-v_4)[2\ln v_4 + \ln u_3] + 2\ln v_4[\ln u_2 + \ln u_3 - \ln u_4] \\ & + \ln u_1 \ln u_2 - \ln u_2 \ln u_4 + \ln u_4 \ln u_1 + 2\zeta_2\,.\end{aligned} \tag{2.14}$$

Due to the correspondence between the form factor and periodic Wilson loops, we can parametrize the kinematics by the coordinates τ_i, σ_i, ϕ_i used in the FFOPE [23–25]. We define

$$T = e^{-\tau}, \quad S = e^{\sigma}, \quad T_2 = e^{-\tau_2}, \quad S_2 = e^{\sigma_2}, \quad F_2 = e^{i\phi_2}. \tag{2.15}$$

The dimensionless ratios u_i, v_i are related to T, S, T_2, S_2, F_2 by

$$\begin{aligned}
u_1 &= \frac{T^2 T_2^2}{(T^2+1)\left(S^2+T^2+T_2^2+1\right)}\,, \\
u_2 &= \left[1+T^2+\frac{S^2[S_2T_2(1+F_2^2)+F_2(1+S_2^2+T^2+T_2^2)]}{F_2S_2^2}\right]^{-1}, \\
u_3 &= \frac{S^2}{(T^2+1)\left(S^2+T^2+T_2^2+1\right)}\,, \\
u_4 &= \frac{S^2T^2}{S_2^2}u_2\,, \\
v_1 &= \frac{T_2^2+1}{S^2+T^2+T_2^2+1}\,, \\
v_2 &= 1+u_2-u_4-v_1\,, \\
v_3 &= 1-u_1+u_3-v_2\,, \\
v_4 &= \frac{T^2}{T^2+1}\,.
\end{aligned} \tag{2.16}$$

2.2 Polylogarithms and (antipodable-)symbol alphabet

We expand the remainder function perturbatively as

$$\mathcal{R}_4 = \sum_{L=2}^{\infty} g^{2L}\mathcal{R}_4^{(L)}\,, \tag{2.17}$$

and similarly for the function $\mathcal{E}_4$. The L-loop quantities $\mathcal{R}_4^{(L)}$ and $\mathcal{E}_4^{(L)}$ are expected to be multiple polylogarithms of weight $2L$.

Multiple polylogarithms (MPLs) are iterated integrals over a logarithmic kernel [54, 65–68]. The total differential of a weight n MPL has the form

$$dF = \sum_{\phi\in\Phi} F^{\phi}\, d\ln\phi\,, \tag{2.18}$$

where the sum is over *letters* ϕ which belong to the *symbol alphabet* Φ, and the ϕ-*coproducts* F^{ϕ} appearing in eq. (2.18) have weight $n-1$. In integral form, MPLs are commonly expressed as G functions,

$$G_{a_1,a_2,\ldots,a_n}(z) = \int_0^z \frac{dt}{t-a_1} G_{a_2,\ldots,a_n}(t)\,, \qquad G_{\underbrace{0,\ldots,0}_{p}}(z) = \frac{\ln^p z}{p!}\,. \tag{2.19}$$

The classical polylogarithms Li_n are special cases of G functions,

$$\mathrm{Li}_n(z) = -G_{\underbrace{0,\ldots,0}_{n-1},1}(z)\,. \tag{2.20}$$

Harmonic polylogarithms (HPLs) [69] $H_{\vec{a}}(z)$ with $a_i \in \{0, 1, -1\}$ are another special case, with

$$H_{\vec{a}}(z) = (-1)^p G_{\vec{a}}(z)\,, \tag{2.21}$$

where p is the number of '1's in the index list $\vec{a}$. Transcendental constants such as multiple zeta values (MZVs) can be viewed as special values of the functions (2.19).

The weight is the number of logarithmic integrations that appear; the weight of a product of polylogarithms is given by the sum of weights of the factors in the product. In the $G_{a_1,\ldots,a_n}(z)$ notation, the weight simply corresponds to the number of indices n.

The symbol [54] of a generic polylogarithmic function F is defined recursively in terms of its total differential (2.18):

$$\mathcal{S}\left(F\right) = \sum_{\phi} \mathcal{S}(F^{\phi}) \otimes \phi\,, \tag{2.22}$$

where $\mathcal{S}(\ln\phi) = \phi$ for letters ϕ by convention. Formally the symbol is also the maximal iteration of the (motivic) coaction Δ associated with a Hopf algebra for MPLs (up to constant entries of the coproduct such as $\ln 2$) [54, 66, 68, 70–72].

The derivatives (2.18) are smooth wherever all the letters in the symbol alphabet Φ are nonvanishing. Conversely, the vanishing loci of the letters ϕ that appear in the tensor product (2.22) provide the locations of possible branch cuts. While the first derivatives are encoded in the last entry of the symbol, according to the iterative definition (2.22), branch cuts can be taken by clipping off suitable first entries. Not all branch cuts are allowed singularities on physical sheets. Requiring only branch cuts at physical locations imposes restrictions on the symbol, called first-entry conditions, and it implies additional restrictions on the function.

The symbol of the four-point $\mathrm{tr}\phi^2$ form factor was first bootstrapped at two loops [49] by starting with a list of 113 symbol letters collected from all the relevant two-loop one-mass five-point integrals [62, 73, 74]. (Note that "planar" $\mathcal{N} = 4$ SYM refers to the leading-color approximation. Non-planar Feynman diagrams can contribute to leading-color form factors of color-singlet operators – provided that the diagram becomes planar when one deletes the external leg corresponding to the operator.) The two-loop symbol only requires 34 out of the 113 letters. The three-loop symbol has been bootstrapped successfully [49] with the assumption that no new letters arise at three loops. It requires 88 out of the 113 letters. If we assume that no new letters arise at higher loops, and we also assume antipodal self-duality at the symbol level, then we find an allowed symbol alphabet of 93 letters. The other 20 of the 113 letters map, under the kinematic map, to functions that are outside of the 113-letter alphabet [75].

This 93-letter "antipodal" alphabet is described in the ancillary file `AntipodalAlphabet.m`.

The alphabet features five square roots $\sqrt{\Delta_{1a}}$, $\sqrt{\Delta_{1b}}$, $\sqrt{\Delta_{2a}}$, $\sqrt{\Delta_{2b}}$, and $\sqrt{\Delta_3}$, where

$$
\begin{aligned}
\Delta_{1a} &= (v_1+v_2)^2 - 4u_2, \\
\Delta_{1b} &= 1 - 2u_1 + {u_1}^2 - 2u_3 - 2u_1u_3 + {u_3}^2, \\
\Delta_{2a} &= {u_1}^2 - 2u_1v_1 + {v_1}^2 + 2{u_1}^2u_2 - 2u_1v_1u_2 + {u_1}^2{u_2}^2 - 2{u_1}^2v_2 + 4u_1v_1v_2 - 2{v_1}^2v_2 \\
&\quad - 2{u_1}^2u_2v_2 + 2u_1v_1u_2v_2 + {u_1}^2{v_2}^2 - 2u_1v_1{v_2}^2 + {v_1}^2{v_2}^2 - 2u_1v_1u_3 + 2{v_1}^2u_3 - 2u_1u_2u_3 \\
&\quad - 2v_1u_2u_3 + 2u_1v_1u_2u_3 - 2u_1{u_2}^2u_3 + 2u_1v_1v_2u_3 - 2{v_1}^2v_2u_3 + 2u_1u_2v_2u_3 + 2v_1u_2v_2u_3 \\
&\quad + {v_1}^2{u_3}^2 - 2v_1u_2{u_3}^2 + {u_2}^2{u_3}^2, \\
\Delta_{2b} &= {u_1}^2{u_2}^2 - 2u_1u_2v_2 - 2{u_1}^2u_2v_2 + 2u_1v_1u_2v_2 + {v_2}^2 + 2u_1{v_2}^2 + {u_1}^2{v_2}^2 - 2v_1{v_2}^2 \\
&\quad - 2u_1v_1{v_2}^2 + {v_1}^2{v_2}^2 - 2u_1u_2u_3 + 2u_1v_1u_2u_3 - 2u_1{u_2}^2u_3 - 2v_2u_3 - 2u_1v_2u_3 + 4v_1v_2u_3 \\
&\quad + 2u_1v_1v_2u_3 - 2{v_1}^2v_2u_3 - 2u_2v_2u_3 + 2u_1u_2v_2u_3 + 2v_1u_2v_2u_3 + {u_3}^2 - 2v_1{u_3}^2 + {v_1}^2{u_3}^2 \\
&\quad + 2u_2{u_3}^2 - 2v_1u_2{u_3}^2 + {u_2}^2{u_3}^2, \\
\Delta_3 &= {u_2}^2 - 2u_1{u_2}^2 + {u_1}^2{u_2}^2 + 2u_1u_2v_2 - 2{u_1}^2u_2v_2 - 2v_1u_2v_2 + 2u_1v_1u_2v_2 + {u_1}^2{v_2}^2 \\
&\quad - 2u_1v_1{v_2}^2 + {v_1}^2{v_2}^2 - 4u_1u_2u_3 + 2v_1u_2u_3 + 2u_1v_1u_2u_3 - 2{u_2}^2u_3 - 2u_1{u_2}^2u_3 \\
&\quad + 2u_1v_1v_2u_3 - 2{v_1}^2v_2u_3 + 2u_1u_2v_2u_3 + 2v_1u_2v_2u_3 + {v_1}^2{u_3}^2 - 2v_1u_2{u_3}^2 + {u_2}^2{u_3}^2 \,.
\end{aligned}
\tag{2.23}
$$

Of the 93 letters, 56 are rational. The other 37 have the form $(a_j + \sqrt{\Delta_m})/(a_j - \sqrt{\Delta_m})$ for some polynomials $a_j(u_i, v_i)$ and $m = 1a, 2a, 1b, 2b, 3$; these 37 letters are odd under some of the Galois symmetries that flip the signs of the various square roots. The form factor should be even under all such Galois symmetries. Flipping the sign of $\sqrt{\Delta_3}$ corresponds to spacetime parity. Antipodal self-duality holds on the parity-preserving surface $\Delta_3 = 0$, which is $F_2 = 1$ in the parametrization (2.16).

Although a complete functional description was already given for the relevant two-loop integrals [62], it was given (so far) only in the kinematical region for $2 \to 3$ scattering where the massive leg has positive mass and is on the outgoing side. We will be interested in other kinematical regions. Also, we wish to extend the description (eventually) to higher loop functions with the same symbol alphabet. Therefore, in the following we will provide an alternate functional description, valid at least for various subspaces of the kinematics. We will focus more on the Euclidean region, which also is relevant for the pseudo-Euclidean region of $1 \to 4$ decay kinematics, where the operator is massive and in the initial state. It would be interesting to connect to the description in refs. [61, 62] in future work.

3 Integrating the symbol up to functions

The two-loop four-gluon form factor has been bootstrapped at the symbol level [49]. At this level, all MZVs vanish, $\mathcal{S}(\text{MZV}) = 0$. In order to describe the form factor at the function level, we need to recover the MZVs. We can do this iteratively in the differential definition (2.18), by providing function-level values for the single coproducts F^ϕ and/or multiple coproducts – which we generically call *P functions* – and by providing boundary values for these quantities

at specific points. On specific surfaces, we can integrate all the way up to the weight 4 $\mathcal{R}_4^{(2)}$ in terms of G functions (or HPLs, for simple enough surfaces).

3.1 Function space

The framework for integrating up the remainder function from lower-weight functions is the coproduct formalism [3, 76]. We construct a set of basis functions, $\{F_i^{(w)}\}$, for each weight w up to $2L$. The sets have dimensions $|F^{(w)}|$ and are big enough to contain all the (multiple) coproducts of the form factor or amplitudes. The different bases are linked to each other by the coproducts $\Delta_{w-1,1}$, which connect two consecutive bases, for weights $w-1$ and w, via a three-index tensor $T_{ij\phi}^{(w)}$:

$$\Delta_{w-1,1} F_i^{(w)} = \sum_{j,\phi} T_{ij\phi}^{(w)} F_j^{(w-1)} \otimes \phi \,. \tag{3.1}$$

Here i, j are indices labelling the basis functions at weight w and $w-1$, respectively; ϕ are letters in the symbol alphabet Φ; $T_{ij\phi}^{(w)}$ are rational numbers filling out a three-index tensor with dimension $|F^{(w)}| \times |F^{(w-1)}| \times |\Phi|$. The symbol-level information corresponds to the coefficients of functions with nonvanishing symbols, whereas the coefficients of MZVs within the $\{F_i^{(w)}\}$ are yet to be fixed. Generally the dimensions $|F^{(w)}|$ have to increase from the symbol-level version, in order to accommodate the MZVs. In our two-loop case, the increase will be very modest, just an increase of one function at weight 2, to account for ζ_2.

This coproduct table effectively defines an iterative differential equation for each basis element,

$$dF_i^{(w)} = \sum_{j,\phi} T_{ij\phi}^{(w)} F_j^{(w-1)} d\ln\phi. \tag{3.2}$$

Once we know the value at any particular point, with the function-level coproduct table, we will be able to integrate up the functions (at least numerically) at an arbitrary kinematic point.

For the description of $\mathcal{R}_4^{(2)}$ we choose a minimal space of P functions with weight up to 4, based on the symbol-level information. At weight 1 we can only have 8 independent functions $\{\ln u_i, \ln v_i\}$, because only these logarithms have branch cuts in the correct location, i.e. the first-entry condition. (We remark that eqs. (2.4)–(2.6) are constraints on the underlying kinematic variables, which do not imply any linear dependence of their logarithms, the symbol letters.) As mentioned above, only 34 of the 93 antipodal letters appear in the two-loop symbol [49]. By taking the iterated $\Delta_{n-1,1}$ coproducts of the symbol $\mathcal{R}_4^{(2)}$, we find that there are 9 independent single coproducts at weight 3 ($\{3,1\}$ coproducts) and 32 independent double coproducts ($\{2,1,1\}$ coproducts). Therefore at symbol level the set of symbols that we need to upgrade to functions consists of 32 at weight two, 9 at weight three, plus 1 weight-four function, $\mathcal{R}_4^{(2)}$ itself.

To fix the beyond-the-symbol constants we make use of the following constraints:

1. **Integrability**: An integrable function must have commuting partial derivatives. Thus if we apply the differential (3.2) twice we need (for variables $x, y \in u_i, v_i$):

$$\frac{\partial^2 F}{\partial x \partial y} = \frac{\partial^2 F}{\partial y \partial x} \,. \tag{3.3}$$

   This condition results in a large set of 3774 independent linear relations among the 93×93 double coproducts F^{ϕ_i,ϕ_j}, which have to hold at function level too.

2. **Physical branch cuts**: The form factor can only develop logarithmic divergences at physical branch points. On the Euclidean sheet, these singularities occur only where the Mandelstam variables s_{ij} or s_{ijk} vanish, or equivalently where u_i or $v_i \to 0$. In other words, any function F in the space has to be nonsingular as $\phi \to 0$ for any letter that is not in the first-entry, $\phi \notin \{u_i, v_i\}$. This condition constrains the first coproducts in particular limits, because derivatives in the singular direction must vanish as $\phi \to 0$.

3. **Extended Steinmann relations**: The BDS-like normalized form factor $\mathcal{E}_4$ should respect the Steinmann relations. The double discontinuity associated with cuts in two overlapping 3-particle channels labeled by $s_{i,i+1,i+2}$ must vanish [49]. (Note that the exponential factor that is removed in eq. (2.9) contains only two-particle invariants.) In terms of the dimensionless letters $v_i = s_{i,i+1,i+2}/q^2$, the following double coproducts vanish

$$F^{v_i,v_j} = 0, \quad i \neq j \,. \tag{3.4}$$

   for the BDS-like normalized function $\mathcal{E}_4$, or any of its coproducts. Strictly speaking, the Steinmann relations only imply eq. (3.4) in the first two slots, i.e. for the weight 2 space $F^{(2)}$. However, in practice we find that this adjacency relation can be applied to all symbol entries in the middle in the two-loop case (but not for v_i, v_{i+2} in the three-loop case). So we could in principle apply $F^{v_i,v_{i+1}} = 0$, everywhere also in the lower-weight functions. However, on the rational surface we use for fixing constants (see Sec. 3.2.1), the limit $u_2 \to v_1 v_2$ means that the association of v_1 and v_2 with 3-particle channels is obscured, and effectively only $F^{v_3,v_4} = 0$ can be used.

4. **Cycle and flip symmetry**: $\mathcal{E}_4$ and $\mathcal{R}_4$ are invariant under the dihedral group D_4, which is generated by the cycle and flip transformations in eqs. (2.7) and (2.8).

5. **Factorization limits**: As described in more detail below, we use universal factorization behavior in soft and collinear kinematic limits, and we match the near-collinear limit to data from the FFOPE.

Taking into account all this information, we are able to fix all the MZVs. We find that ζ_2 needs to be added as an independent weight-2 function, while ζ_3 can be absorbed into the existing 9 weight 3 symbol-level coproducts. Therefore the spaces of functions needed to describe $\mathcal{R}_4^{(2)}$ have dimensions $|F^{(1)}| = 8$, $|F^{(2)}| = 33$, $|F^{(3)}| = 9$, $|F^{(4)}| = 1$. Our result for the iterated coproduct table at function level is contained in the ancillary file `R42funcCoTable.m`.

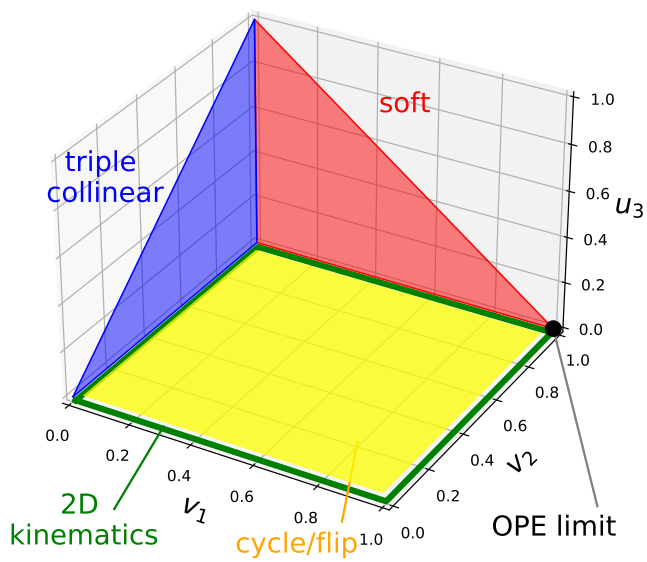

Figure 1: The rational surface is parametrized by three kinematic variables (u_3, v_1, v_2). It intersects a soft limit at the $v_2 = 1$ surface (red). The intersection with a triple collinear limit is at the $v_1 = 0$ surface (blue). The $u_3 = 0$ surface (yellow) maps into itself under two dihedral transformations $\mathcal{C}^2$ and $\mathcal{C} \cdot \mathcal{F}$, as indicated by "cycle/flip". The (green) square boundary of the $u_3 = 0$ surface intersects another two-parameter surface (3.23) where the momenta all lie in two spacetime dimensions. The point $(0, 1, 1)$ makes contact with the OPE limit.

3.2 Boundary kinematics

We first consider a three-parameter rational surface where the symbol alphabet simplifies so that all letters are rational functions of u_3, v_1, v_2. This surface also interpolates between soft, collinear, OPE, multi-Regge, and self-crossing limits. Using these limits, we can deduce the G-function representation of the remainder function on the rational surface, $\mathcal{R}_4^{(2)}(u_3, v_1, v_2)$. This representation automatically gives zeta-valued information for coproducts corresponding to derivatives in directions tangent to the rational surface. However, other coproducts are needed for derivatives along directions normal to the rational surface. To determine them, we use bulk conditions such as integrability. In this way, we can recover the function-level information for the full coproduct table in the bulk. Given the expressions for all the basis functions $F_i^{(w)}$ (the P functions) on the rational surface boundary, the function in the bulk is uniquely defined. We illustrate the rational surface, and how it connects different kinematic limits, in Fig. 1.

3.2.1 Rational surface and soft/collinear factorization

The rational surface is defined by the limit

$$\frac{u_2}{v_1 v_2} \to 1, \qquad u_1 \to 0, \tag{3.5}$$

with u_3, v_1, v_2 generic. On this surface, the 93-letter antipodal symbol alphabet simplifies to the following 20 letters:

$$\begin{aligned}\Phi_{\text{rational}} = \big\{&u_3, \quad v_1, \quad v_2, \quad 1-u_3, \quad 1-v_1, \quad 1-v_2, \quad 1+u_3, \quad u_3+v_1,\\ &-u_3+v_2, \quad v_1-v_2, \quad 1-u_3-v_1, \quad 1+u_3-v_2, \quad u_3+v_1-v_2,\\ &-u_3+v_2-v_1v_2, \quad u_3+v_1-v_1v_2, \quad -u_3+u_3v_1+v_2-v_1v_2-u_3v_1v_2,\\ &-u_3+v_2-2v_1v_2+u_3v_1v_2+v_1^2v_2, \quad -u_3v_1-u_3v_2+u_3v_1v_2+v_2^2-v_1v_2^2,\\ &u_3+v_1-2v_1v_2-u_3v_1v_2+v_1v_2^2, \quad u_3v_1+v_1^2+u_3v_2-u_3v_1v_2-v_1^2v_2\big\}.\end{aligned} \tag{3.6}$$

All the letters are now rational (polynomial) in u_3, v_1, v_2. There is also the trivial infinitesimal letter u_1, which factors out on the rational surface, i.e. all functions are polynomial in $\ln u_1$. Furthermore, at two loops the last four letters do not appear and the alphabet becomes *linearly reducible* [77], thus enabling us to conveniently represent $\mathcal{R}_4^{(2)}$ in terms of G-functions in this limit.

We remark that at three loops, although three of the last four letters in eq. (3.6) appear in the symbol, they never appear together in the same symbol term. This feature allows for some contributions to be linearized in v_1, and others in v_2, so that a representation of the 3-loop remainder function in terms of G-functions with rational arguments appears feasible as well.

Given the symbol, the function-level result on the rational surface can be fully determined by the physical branch cut conditions, cycle-flip symmetry, and soft/collinear limits, as we shall now discuss.

First, we discuss the branch-cut conditions. In the rational alphabet (3.6) the letters at two loops that do not correspond to physical Mandelstam variables (taking into account $u_2 = v_1v_2$, $u_4 = (1-v_1)(1-v_2)$, etc.) are

$$\begin{aligned}&1-u_3, \quad 1+u_3, \quad u_3+v_1, \quad -u_3+v_2, \quad v_1-v_2, \quad u_3+v_1-v_2,\\ &-u_3+v_2-v_1v_2, \quad u_3+v_1-v_1v_2, \quad -u_3+u_3v_1+v_2-v_1v_2-u_3v_1v_2.\end{aligned} \tag{3.7}$$

These letters ϕ should not give rise to singularities of form factors. That is, $\mathcal{R}_4^{(2)}$ and its coproducts should be finite as $\phi \to 0$, where ϕ are the letters in eq. (3.7). We have observed this at the symbol level, where the finiteness is due to letters preceding ϕ going to 1 as $\phi \to 0$, which leads to power-law vanishing in this region. At the function level, we need to remove all zeta-value containing functions that have unphysical branch cuts, e.g. $\zeta_2 \ln \phi$ behavior for any coproduct F as $\phi \to 0$. So we require that $F^\phi \to 0 \times \zeta_2$ in this region (and similarly with ζ_3 at weight 3).

Secondly, we discuss consequences of dihedral symmetry. The rational surface (3.5) can be related to another rational surface, $\frac{u_2}{v_1v_2} \to 1, u_3 \to 0$, by a cycle-then-flip transformation,

$$\mathcal{F}\cdot\mathcal{C}: \quad p_1 \leftrightarrow p_4, \quad p_2 \leftrightarrow p_3 \quad \Rightarrow \quad u_1 \leftrightarrow u_3, \quad v_1 \leftrightarrow v_2, \quad v_3 \leftrightarrow v_4\,. \tag{3.8}$$

These two dihedral images of the rational surface make contact at a sub-limit of the first surface, $u_3 \to 0$. Therefore, the two-parameter surface parametrized by v_1, v_2 at

$$\frac{u_2}{v_1 v_2} \to 1, \quad u_1 \to 0, \quad u_3 \to 0 \tag{3.9}$$

is mapped to itself through the reflection (3.8) which exchanges $v_1 \leftrightarrow v_2$. In fact, the symbol of $\mathcal{R}_4^{(2)}(u_3, v_1, v_2)$ vanishes at the rational surface boundary $u_3 \to 0$. We find, after implementing other constraints, that $\mathcal{R}_4^{(2)}(u_3, v_1, v_2)$ also vanishes at function level for $u_3 \to 0$. So the way the dihedral symmetry of $\mathcal{R}_4^{(2)}$ is implemented on this boundary is rather trivial, $0 \leftrightarrow 0$.

Thirdly, there are a few other sub-limits where the behavior of $\mathcal{R}_4^{(2)}$ is known by soft-collinear factorization. The soft limit of the external momentum $p_1 \to 0$ is contained inside the rational surface as $v_2 \to 1$. In this soft limit, the four-point form-factor remainder function goes smoothly into the three-point form factor,

$$\mathcal{R}_4^{(2)}|_{\text{rational},\, v_2 \to 1} \quad \to \quad \mathcal{R}_3^{(2)} \,. \tag{3.10}$$

The right-hand side is known at function level for general kinematics [78]:

$$\begin{aligned}\mathcal{R}_3^{(2)}(u,v) = &-2\left[\mathrm{J}_4\left(-\frac{uv}{w}\right) + \mathrm{J}_4\left(-\frac{vw}{u}\right) + \mathrm{J}_4\left(-\frac{wu}{v}\right)\right] - 8\sum_{i=1}^{3}\left[\mathrm{Li}_4\left(1 - x_i^{-1}\right) + \frac{\log^4 x_i}{4!}\right] \\ &- 2\left[\sum_{i=1}^{3}\mathrm{Li}_2(1 - x_i^{-1})\right]^2 + \frac{1}{2}\left[\sum_{i=1}^{3}\log^2 x_i\right]^2 - \frac{\log^4(uvw)}{4!} - \frac{23}{2}\zeta_4 \,,\end{aligned} \tag{3.11}$$

with

$$\mathrm{J}_4(z) = \mathrm{Li}_4(z) - \log(-z)\mathrm{Li}_3(z) + \frac{\log^2(-z)}{2!}\mathrm{Li}_2(z) - \frac{\log^3(-z)}{3!}\mathrm{Li}_1(z) - \frac{\log^4(-z)}{48} \,, \tag{3.12}$$

where $x_1 = u = \frac{s_{12}}{s_{123}}$, $x_2 = v = \frac{s_{23}}{s_{123}}$ and $x_3 = w = 1 - u - v = \frac{s_{31}}{s_{123}}$ are the dimensionless ratios parametrizing the three-point form factor. They are related to the u_i, v_i variables in the four-point form factor in the soft limit by

$$u = v_1, \quad v = u_3, \quad w = 1 - v_1 - u_3. \tag{3.13}$$

In other words, the rational surface soft limit is fixed at function level by $\mathcal{R}_4^{(2)}(u_3, v_1, 1) = \mathcal{R}_3^{(2)}(v_1, u_3) = \mathcal{R}_3^{(2)}(u_3, v_1)$, using also the D_3 dihedral symmetry of $\mathcal{R}_3$.

Fourthly, another sub-kinematics inside the rational surface is the triple collinear limit where three external momenta are parallel. In OPE variables this corresponds to letting $T \to 0$, for a parametrization like eq. (2.16) but after cycling $u_i \to u_{i+1}$, $v_i \to v_{i+1}$. The remainder function $\mathcal{R}_4^{(2)}$ in this limit, at leading power in T, reduces smoothly to the remainder function of the MHV six-gluon scattering amplitude $R_6^{(2)}$ [49]. This result follows from dual conformal invariance and factorization [39], and it can also be seen in the FFOPE framework [23–26]. The three-parameter rational surface makes contact with the triple collinear limit on a two-parameter surface at $v_1 \to 0$. (Note that two of the two-particle invariants vanish as well in

this rational-surface limit, u_1 and $u_2 = v_1 v_2$.) The six-point remainder function in this limit is:

$$\begin{aligned}\lim_{\hat{v}\to 1,\hat{w}\to 0} R_6^{(2)}(\hat{u},\hat{v},\hat{w}) = {} & \ln\hat{w}\big[2\mathrm{Li}_3(\hat{u}) - \ln\hat{u}\mathrm{Li}_2(\hat{u})\big] - 4\mathrm{Li}_4(\hat{u}) + 2\mathrm{Li}_4\left(\frac{-\hat{u}}{1-\hat{u}}\right) - \frac{1}{2}\big[\mathrm{Li}_2(\hat{u})\big]^2 \\ & + \ln\hat{u}\left[2\mathrm{Li}_3(\hat{u}) - \ln(1-\hat{u})\mathrm{Li}_2(\hat{u}) - \frac{1}{3}\ln^3(1-\hat{u})\right] + \frac{1}{12}\ln^4(1-\hat{u}) \\ & + \zeta_2\big[2\mathrm{Li}_2(\hat{u}) + \ln^2(1-\hat{u})\big]\,, \end{aligned} \tag{3.14}$$

where $\hat{u} = \frac{s_{12}s_{45}}{s_{123}s_{345}}$, $\hat{v} = \frac{s_{23}s_{56}}{s_{234}s_{456}}$, $\hat{w} = \frac{s_{34}s_{61}}{s_{345}s_{561}}$ are cross ratios describing the six-gluon kinematics. They are related to the u_i, v_i describing the four-point form factor by

$$\hat{u} = \frac{u_3(1-v_2)}{v_2(1-u_3)}, \quad \hat{w} = \frac{u_1}{v_1(1-u_3)}, \quad \text{with } u_1 \ll v_1. \tag{3.15}$$

In summary, the triple-collinear boundary condition is $\mathcal{R}_4^{(2)}(u_3, v_1, v_2)|_{v_1\to 0} = R_6^{(2)}(\hat{u}, 1, \hat{w})$, where $\hat{u}, \hat{w}$ are given in eq. (3.15).

These constraints fully determine the remainder function on the rational surface at function level. On this surface, the remainder function has a mild logarithmic singularity due to the fact that $u_1 \to 0$:

$$\mathcal{R}_4^{(2)}(u_1; u_3, v_1, v_2) = D_0(u_3, v_1, v_2) + D_1(u_3, v_1, v_2)\ln u_1\,. \tag{3.16}$$

The coefficient of $\ln u_1$ is a weight 3 MPL,

$$
\begin{aligned}
D_1 = {} & 4\zeta_2\Big[G_0(1-v_1) + G_0(1-v_2) - G_1(v_2) + G_{1-v_1}(u_3) - G_0(1-v_1-u_3)\Big] \\
& + \Big(G_0(v_2) - G_1(v_2)\Big)\Big[G_{-v_1,-1}(u_3) + G_{-v_1,1-v_1}(u_3) - G_{1-v_1,1-v_1}(u_3) + G_{v_2,v_2}(u_3) \\
& \qquad + G_{v_2,-1+v_2}(u_3) - 2G_{0,v_2}(u_3) - G_{0,-1}(u_3) + G_{1-v_1,v_2}(u_3) + G_{v_2,1-v_1}(u_3) \\
& \qquad - G_{-v_1+v_2,1-v_1}(u_3) - G_{-v_1+v_2,-1+v_2}(u_3) \\
& \qquad + G_{0,(1-v_1)v_2/(1-v_1+v_1v_2)}(u_3) - G_{v_2,(1-v_1)v_2/(1-v_1+v_1v_2)}(u_3)\Big] \\
& - 4G_{0,1,0}(u_3) + 2\Big[G_{0,1-v_1,0}(u_3) + G_{1-v_1,1,0}(u_3) + G_{0,v_2,0}(u_3) + G_{v_2,1,0}(u_3) \\
& + G_{0,v_2,-1+v_2}(u_3) - G_{v_2,-1+v_2,-1+v_2}(u_3) + G_{-v_1+v_2,-1+v_2,-1+v_2}(u_3)\Big] - G_{0,-1,0}(u_3) \\
& + G_{-v_1,-1,0}(u_3) + G_{-v_1,1-v_1,0}(u_3) + G_{-v_1,1-v_1,1-v_1}(u_3) - G_{1-v_1,1-v_1,0}(u_3) \\
& - G_{1-v_1,1-v_1,1-v_1}(u_3) - G_{v_2,v_2,0}(u_3) - G_{v_2,v_2,-1+v_2}(u_3) + G_{0,-1,-1+v_2}(u_3) \\
& + G_{v_2,-1+v_2,0}(u_3) + G_{v_2,0,-1+v_2}(u_3) - G_{0,-v_1+v_2,1-v_1}(u_3) - G_{0,-v_1+v_2,-1+v_2}(u_3) \\
& - G_{-v_1,-1,-1+v_2}(u_3) - G_{-v_1,-v_1+v_2,1-v_1}(u_3) - G_{-v_1,-v_1+v_2,-1+v_2}(u_3) - G_{1-v_1,v_2,0}(u_3) \\
& - G_{1-v_1,v_2,-1+v_2}(u_3) + G_{1-v_1,-v_1+v_2,1-v_1}(u_3) + G_{1-v_1,-v_1+v_2,-1+v_2}(u_3) + G_{v_2,0,1-v_1}(u_3) \\
& - G_{v_2,1-v_1,0}(u_3) - G_{v_2,1-v_1,-1+v_2}(u_3) - G_{v_2,-1+v_2,1-v_1}(u_3) + G_{v_2,-v_1+v_2,1-v_1}(u_3) \\
& + G_{v_2,-v_1+v_2,-1+v_2}(u_3) - G_{-v_1+v_2,0,1-v_1}(u_3) - G_{-v_1+v_2,1-v_1,0}(u_3) - G_{-v_1+v_2,0,-1+v_2}(u_3) \\
& - G_{-v_1+v_2,-1+v_2,0}(u_3) + G_{-v_1+v_2,1-v_1,-1+v_2}(u_3) + G_{-v_1+v_2,-1+v_2,1-v_1}(u_3) \\
& - G_{0,(1-v_1)v_2/(1-v_1+v_1v_2),0}(u_3) + G_{v_2,(1-v_1)v_2/(1-v_1+v_1v_2),0}(u_3) \\
& + G_{0,(1-v_1)v_2/(1-v_1+v_1v_2),1-v_1}(u_3) - G_{v_2,(1-v_1)v_2/(1-v_1+v_1v_2),1-v_1}(u_3)\,.
\end{aligned}
\tag{3.17}
$$

The weight 4 function D_0 is more complicated, but we provide $\mathcal{R}_4^{(2)}(u_1; u_3, v_1, v_2)$ in terms of G-functions in the ancillary file `R42_rational.m`. The basis of lower-weight functions appearing in the coproducts of $\mathcal{R}_4^{(2)}$ is given on the rational surface in the ancillary file `Prat.m`.

3.2.2 FFOPE limit: Near multi-collinear factorization

In the multi-collinear limit, scattering amplitudes and form factors are expected to factorize into splitting amplitudes and lower-multiplicity amplitudes and/or form factors (see e.g. ref. [39]). For the four-point form factors the kinematical limits can be expressed in terms of the OPE variables as $T \to 0$ and/or $T_2 \to 0$. The limit $T \to 0$ corresponds to the triple collinear limit where p_4, p_1, p_2 are all parallel ($p_4 \parallel p_1 \parallel p_2$), which sends $v_4, u_4, u_1 \to 0$. The limit $T_2 \to 0$ corresponds to the ordinary collinear limit $p_1 \parallel p_2$, which sends $u_1 \to 0$ [49].

The triple collinear limit, where the form factor is related to the MHV six-gluon amplitude (3.14), has already been used to give boundary information for the remainder function on the rational surface. The ordinary collinear limit, like the soft limit, reduces the four-point form factor down to a three-point form factor (3.11). Moreover, it has recently been shown,

at symbol level, that these multi-collinear limits relate an antipodal self-duality for $\mathcal{R}_4$ to the duality between the MHV six-point amplitude and the three-point form factor [49].

We now consider the double series expansion in both T and T_2. The power series in T_2 at leading T^0 order corresponds to the OPE expansion of the six-gluon amplitude found in the triple-collinear limit. The power series of T at leading T_2^0 order corresponds to the FFOPE expansion of the three-point form factor found in the ordinary collinear limit. Additional information is provided by the terms with positive powers of both T and T_2. They are predicted by the four-point [FF]OPE framework [17–22, 26, 79–85], more specifically refs. [23–25, 86].

In the OPE limit, the symbol alphabet, written in terms of the OPE variables, simplifies to

$$\Phi_{\text{OPE}} = \big\{S, \quad S_2, \quad S^2+1, \quad S_2^2+1, \quad S^2S_2^2+S^2+S_2^2, \quad S^4S_2^2+S^4+2S^2S_2^2+S_2^2\big\}. \tag{3.18}$$

There are also the infinitesimal letters T and T_2, which just generate powers of the logarithms $\ln T$ and $\ln T_2$. To make the alphabet (3.18) *linearly reducible* [77], we find it convenient to use the variables

$$X = \frac{S^2}{1+S^2}, \quad Y = \frac{S_2^2}{1+S_2^2}, \tag{3.19}$$

so that the alphabet becomes

$$\Phi_{XY} = \big\{X, \quad Y, \quad 1-X, \quad 1-Y, \quad X+Y-XY, \quad X^2+(1-X^2)Y\big\}, \tag{3.20}$$

which is linearly reducible in the $\{Y, X\}$ basis.

We note that although Φ_{XY} appears to contain X^2, after integrating in Y, the quadratic dependence on X drops out. More specifically, we follow the fibration algorithm described in refs. [77, 87]. After integration in Y, the alphabet in the next iteration is

$$\Phi_{XY}^{(Y)} \equiv \{QR'-RQ'|(QY+R)\in\Phi_{XY}, (Q'Y+R')\in\Phi_{XY}\} = \{X, 1-X, 1+X\}, \tag{3.21}$$

and this is linear in X. For instance, take the two letters $X+Y-XY$ and $X^2+(1-X^2)Y$. They contain X^2 but only contribute to $\Phi_{XY}^{(Y)}$ as $(1-X)X^2 - X(1-X^2) = -X(1-X)$.

Exploiting the linearity, we are able to integrate up around the OPE limit and fix the function-level information for the basis P functions for the coproducts of $\mathcal{R}_4^{(2)}$, iteratively in the weight, by performing similar procedures as we did for the rational surface limit.

However, for higher powers of T and T_2 in the OPE limit, we need to fix more constants in the coproducts than were needed for the rational surface. In order to fix them, we used a combination of dihedral symmetry constraints (see Sec. 3.3) and matching to the FFOPE data. The ancillary file `PTT2to0_XY.m` contains the G-function representation of these basis functions in the OPE limit, at leading power in T and T_2. It contains the constants needed for taking derivatives in the full five-dimensional phase space.

We have also constructed all these functions at higher orders in T and T_2, through order $T^2T_2^2$. At weight 4, we obtain the OPE limit of $\mathcal{R}_4^{(2)}$ itself. The OPE expansion of the

remainder function for terms with positive powers of both T and T_2, through order $T^2T_2^2$, has the form:

$$\begin{aligned}\mathcal{R}_4^{(2)} = T^2\Big\{ & T_2(F_2+F_2^{-1})\Big(\ln T\, A_{1,1} + \ln T_2\, A_{1,2} + A_{1,3} + \zeta_2 A_{1,4}\Big) \\ & + T_2^2\Big[(F_2^2+F_2^{-2})\Big(\ln T\, A_{2,2,1} + \ln T_2\, A_{2,2,2} + A_{2,2,3} + \zeta_2 A_{2,2,4}\Big) \\ & \qquad + \ln T\, A_{2,0,1} + \ln T_2\, A_{2,0,2} + A_{2,0,3} + \zeta_2 A_{2,0,4}\Big]\Big\} \;+\; \mathcal{O}(T^2T_2^3)\,.\end{aligned} \tag{3.22}$$

The A coefficients depend only on S, S_2 (or $x = S^2, y = S_2^2$). They are given in Appendix A. We expose the beyond-the-symbol terms containing ζ_2 explicitly as $A_{1,4}$, $A_{2,2,4}$, $A_{2,0,4}$. To compare with the FFOPE results [86], which are provided as a series expansion around $S \to 0$, $1/S_2 \to 0$, we also perform this straightforward series expansion. The available FFOPE components are $A_{1,i}$, $i = 1, 2, 3, 4$; $A_{2,2,1}$, $A_{2,2,2}$, and $A_{2,0,2}$. They all agreed perfectly with the series expansions of our results.

3.2.3 2D kinematics

When the external momenta are constrained to lie in two spacetime dimensions, the corresponding periodic Wilson loop has been computed at strong coupling [41]. Here we consider the weak-coupling value. In terms of Mandelstam variables, this limit is parametrized by

$$\begin{aligned} & u_1 = v_1(1-v_2), \quad u_2 = v_1 v_2, \quad u_3 = (1-v_1)v_2, \quad u_4 = (1-v_1)(1-v_2), \\ & v_3 = 1-v_1, \quad v_4 = 1-v_2\,. \end{aligned} \tag{3.23}$$

The symbol alphabet in this limit simplifies to

$$\Phi_{2\mathrm{D}} = \big\{v_1,\ v_2,\ 1-v_1,\ 1-v_2,\ 1-v_1-v_2,\ v_1-v_2\big\}. \tag{3.24}$$

(In principle, the alphabet could also contain the letters $1+v_1-v_2$ and $1-v_1+v_2$, but they cancel in the symbol of the remainder function.)

The 2D kinematics make contact with the rational surface (and its dihedral image) on the four one-parameter line segments $v_1 = 0$, $v_1 = 1$, $v_2 = 0$, and $v_2 = 1$. These segments form a square boundary of the region $0 \le v_1, v_2 \le 1$. One of the segments, $v_2 = 1$, is a one-parameter subspace of the $p_1 \to 0$ soft limit, where the behavior of $\mathcal{R}_4^{(2)}$ is specified by a limit of eq. (3.11). Another segment, $v_1 = 0$, is a subspace of the triple-collinear limit, where the behavior of the remainder function is dictated by a limit of eq. (3.14).

Furthermore, this square parametrized by (v_1, v_2) is mapped into itself by the bulk cyclic transformation $\mathcal{C}$. Projected onto this surface, the transformation is

$$\mathcal{C}: \quad v_1 \to v_2 \to (v_3 = 1-v_1) \to (v_4 = 1-v_2) \to v_1, \tag{3.25}$$

$$\mathcal{C}^2: \quad v_1 \leftrightarrow 1-v_1, \quad v_2 \leftrightarrow 1-v_2. \tag{3.26}$$

We require this dihedral symmetry of the remainder function to hold at function level for 2D kinematics.

Based on these constraints, we can fully recover the function-level information in 2D kinematics. The remainder function in this limit can be expressed in terms of G-functions of v_1, v_2. The detailed expression is given in Appendix B.

3.3 Dihedral symmetry constraints

We have made heavy use of dihedral symmetry in the evaluation of the remainder function in the aforementioned boundary kinematics. We have further used the information from the cycle/flip symmetry that connects different boundaries, in order to fix $\mathcal{R}_4^{(2)}$ in the bulk. That is, we provide constants for all the lower-weight coproducts required to integrate up $\mathcal{R}_4^{(2)}$ off the rational surface at function level. In the OPE parametrization, near the OPE limit, the constants are provided via the ancillary file `PTT2to0_XY.m`. In the cross-ratio parametrization on the rational surface, the constants are provided via the ancillary file `Prat.m`.

The rest of this subsection collects how various dihedral symmetries act in relevant limits.

In the OPE limit, there is a one-parameter line parametrized by S in the limit that $S_2 = \frac{1}{T_2} \to \infty$. The flip transformation $\mathcal{F}$ in eq. (2.8) is represented on this line by

$$\mathcal{F}: \quad S \to \frac{1}{S}. \tag{3.27}$$

As mentioned above, there is a two-parameter subsurface (3.9) of the rational surface, which is mapped to itself by the reflection (3.8). It is also mapped to itself by the $\mathcal{C}^2$ symmetry (the cycle symmetry (2.7) applied twice). In this limit, $\mathcal{C}^2$ acts as

$$u_1 \leftrightarrow u_3, \quad v_1 \leftrightarrow 1 - v_2\,. \tag{3.28}$$

Compare this with the $\mathcal{C}^2$ symmetry in 2D kinematics, eq. (3.26). They are compatible because the intersection has either $v_1, v_2 \to 0$ or $v_1, v_2 \to 1$, so $v_1 \approx v_2$ in both cases.

The rational surface and the OPE limit make contact at one kinematic point, namely $(u_1, u_2, u_3, v_1, v_2) = (0, 1, 0, 1, 1)$. In the OPE parametrization, however, this point is actually a line in the limit $T, T_2, S \to 0$, which is parametrized by S_2. In terms of the cross ratios u_i, v_i, the variable S_2 parametrizes how fast $u_3 \to 0$ compared to $v_2 \to 1$. The relation between the OPE variables and u_i, v_i in this limit is

$$u_1 \to T^2 T_2^2, \quad u_3 \to S^2, \quad v_1 \to 1 - T^2, \quad v_2 \to 1 - \frac{S^2}{S_2^2}\,, \tag{3.29}$$

where S_2 is finite and T, T_2, S are small. Hence $u_3/(1 - v_2) \to S_2^2$.

The cycle-then-flip symmetry (3.8), which maps the $u_3 \to 0$ rational surface to the $u_1 \to 0$ rational surface, is also preserved near this kinematic point (or the line parametrized by S_2).

4 Remainder function in the bulk

In this section, we give numerical results on several slices through the rational surface. We also check the proposed antipodal self-duality [49] at the function level, by comparing the ζ_3 parts of the derivatives (or $\{3, 1\}$ coproducts) and the branch cuts (to obtain the antipodally related $\{1, 3\}$ coproducts).

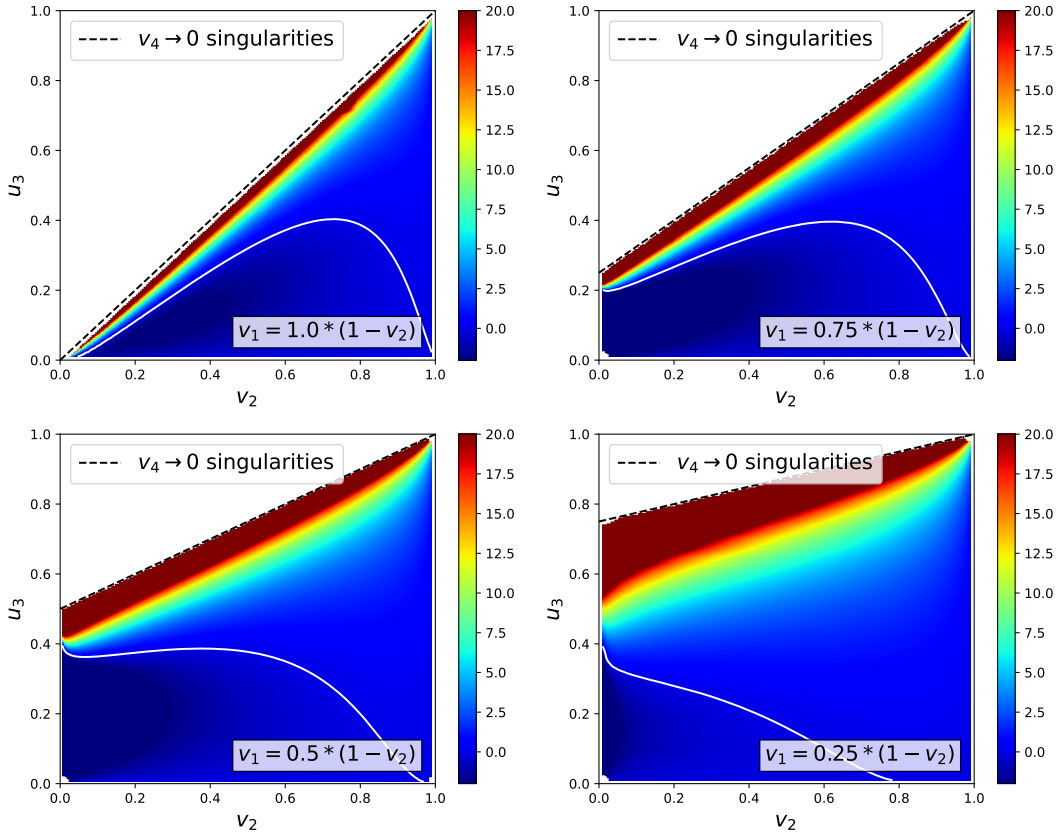

Figure 2: The finite part $D_0(u_3, v_1, v_2)$ of the remainder function $\mathcal{R}_4^{(2)}$ on the $v_1 = k(1 - v_2)$ slice with the constant $k = 0.25,\ 0.5,\ 0.75,\ 1$. The white curves highlight where $\mathcal{R}_4^{(2)}$ flips sign.

4.1 Slices through the rational surface

We present numerical values of $\mathcal{R}_4^{(2)}$ in the three-parameter rational surface kinematics introduced in Sec. 3.2.1 by evaluating them on several two-parameter slices through this surface. As mentioned in Sec. 3, $\mathcal{R}_4^{(2)}$ has a mild (linear) logarithmic singularity in u_1 on the rational surface, $\mathcal{R}_4^{(2)}|_{\text{rat.}} = D_0 + D_1 \ln u_1$, as given in eq. (3.16). In Figs. 2 and 3, we plot the finite part $D_0(u_3, v_1, v_2)$ as a function of u_3 and v_2, on slices parametrized by $v_1 = k(1 - v_2)$, for different values of the constant k. We see that the remainder function is smooth inside this region and diverges only near a physical singularity, indicated by the dashed line at $u_3 = 1 - k(1 - v_2)$, where the variable $v_4 \to 0$.

4.2 Antipodal duality beyond the symbol

Antipodal duality between the three-point form factor and the MHV six-gluon amplitude has been verified well beyond the level of the symbol [48]. Because the right-hand side of the coaction is only defined modulo $i\pi$ (and any powers thereof), at present all the checks have

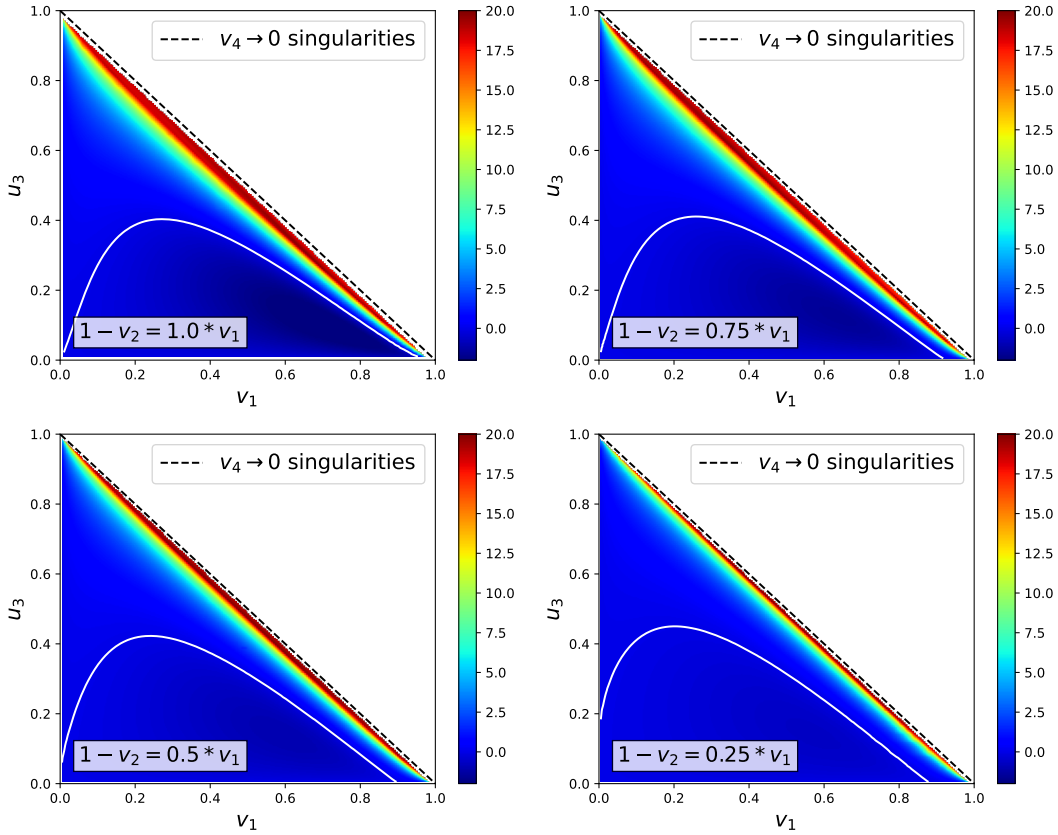

Figure 3: The finite part of the remainder function $\mathcal{R}_4^{(2)}$ on the $v_1 = k(1 - v_2)$ slice when $k \geq 1$.

been modulo $i\pi$. This still leaves a large number of beyond-the-symbol checks that have been passed. For example, at dual points where the three-point form factor and the MHV six-gluon amplitude evaluate to MZVs, in the f-alphabet representation [88, 89] of the MZV's, the values of the multi-loop form factor and amplitude are related to each other by dropping all π-containing terms and reversing the order of all the f letters, through eight loops [15, 48].

On the other hand, the antipodal self-duality of the four-point form factor has only been checked so far at the symbol level [49], since the function is only now available. We want to show invariance under the antipode map, reversing the symbol and the various coactions, combined with the *kinematic map*:

$$T \to \sqrt{\frac{T_2}{S_2}}\,, \qquad S \to \sqrt{\frac{1}{T_2 S_2}}\,, \qquad T_2 \to \frac{T}{S}\,, \qquad S_2 \to \frac{1}{TS}\,, \tag{4.1}$$

Because antipodal duality holds between the three-point form factor and the MHV six-gluon amplitude including multiple zeta values, and because these two functions are limits of the four-point form factor, it would be surprising if antipodal-self-duality failed for $\mathcal{R}_4^{(2)}$ at the function level. Still, we should check it.

At two loops, or weight four, there is not too much that can be checked beyond the symbol level, given the modulo $i\pi$ constraint. The only constant at or below weight four, that does not vanish modulo $i\pi$, is ζ_3. There are two ways that ζ_3 can appear in the coaction:

1. In the $\{3,1\}$ part of the coaction, one can go to a particular point where the weight three function evaluates to ζ_3, and look for terms of the form $c\,\zeta_3 \otimes \ln\phi'$, where ϕ' is a symbol letter (that appears as a final entry).

2. In the $\{1,3\}$ part of the coaction, one can look for terms of the form $c\,\ln\phi \otimes \zeta_3$, where ϕ is a symbol letter (that appears as an initial entry).

To perform the function level check at two loops, we simply need to show that these two types of terms map into each other under the antipode, which exchanges $\{3,1\} \leftrightarrow \{1,3\}$, and under the kinematic map, which should exchange letters $\phi \leftrightarrow \phi'$, while keeping the constant prefactors c the same.

In fact we will show that this duality of ζ_3 terms holds by mapping vanishing constant prefactors to each other, $c = 0$. This happens at the *OPE limit* point where $(u_1, u_2, u_3, v_1, v_2) = (0, 1, 0, 1, 1)$. This point is a fixed point of the kinematic map (4.1), when we take $T, T_2 \to 0$, and $S \to 0$, $S_2 \to \infty$. To see this, we can let $T \propto T_2^2$, $S \propto T_2$, $S_2 \propto 1/T_2^3$. Then both sides of the map (4.1) scale the same way as $T_2 \to 0$.

At the OPE limit point, as discussed in Sec. 3.2.2, $\mathcal{R}_4^{(2)}$ vanishes at leading power in T, T_2. In addition, inspection of all of the $\{3,1\}$ coproducts at the OPE limit point, using the ancillary file `PTT2to0_XY.m`, shows that none of them contains a ζ_3. Such a ζ_3 controls derivatives around the OPE limit point, and so it would also have shown up in the OPE expansion (A.1). Thus there is no $\zeta_3 \ln(\phi')$ term for any letter ϕ'. Also, at the OPE limit point u_1, u_3, u_4, v_3, v_4 all vanish, and so the logarithms of these five letters have branch cuts originating there. Therefore we also know that the $\{1,3\}$ coproducts $\ln\phi \otimes \zeta_3$ have vanishing coefficient for $\phi \in \{u_1, u_3, u_4, v_3, v_4\}$; otherwise we would see a logarithmic singularity in $\mathcal{R}_4^{(2)}$ at the OPE limit point, directly on the edge of the Euclidean sheet.

The task of this subsection is to show that the constants in $c\,\ln\phi \otimes \zeta_3$ for the other three first entries, $\phi \in \{u_2, v_1, v_2\}$, also vanish. Because $u_2, v_1, v_2 \to 1$ at the OPE limit point, the logarithms vanish there. In order to reveal these discontinuities, we need to connect the OPE limit point with limits where u_2, v_1 or v_2 vanishes.

First we consider $\phi = u_2$. We reveal the potential $\ln u_2 \otimes \zeta_3$ term by considering a one-dimensional path in the phase-space which is parametrized by u_2 and which extends out of the rational surface:

$$\mathscr{P}: \; u_1, u_3 \to 0, \quad v_1, v_2 \to 1, \quad 0 < u_2 < 1. \tag{4.2}$$

Along this path $\mathscr{P}$, shown in Fig. 4, the symbol alphabet simplifies to $\{\eta, 1+\eta, 1-\eta\}$ with $\eta = \sqrt{1-u_2}$, i.e. the u_2 dependence becomes HPLs of η with indices $a_i \in \{0, 1, -1\}$. The following logarithms are divergent on this path $\mathscr{P}$: $\{\ln u_1, \ln u_3, \ln(1-v_1), \ln(1-v_2)\}$.

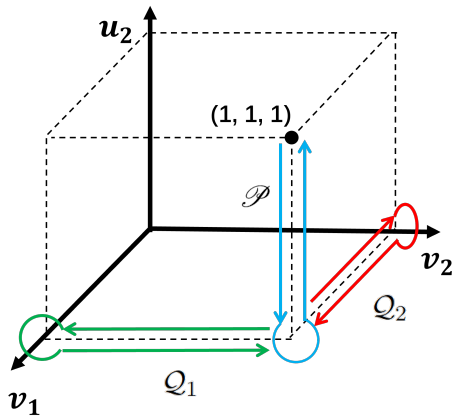

Figure 4: Diagram showing paths along which we integrate to obtain the u_2, v_1, v_2 discontinuities of $\mathcal{R}_4^{(2)}$.

Any term with one of these divergent logarithms cannot contribute to the $\ln u_2 \otimes \zeta_3$ term, because it would have to have a total weight of at least five, and $\mathcal{R}_4^{(2)}$ only has weight four. Thus we only need to keep track of the finite part, which we compute to be:

$$\begin{aligned}
&\mathcal{R}_4^{(2)}|_{u_1,u_3\to 0, v_1,v_2\to 1,\,\text{finite part}} \\
&\quad = -4H_{-1,-1,0,-1}(\eta) + 4H_{-1,-1,0,0}(\eta) + 4H_{-1,-1,0,1}(\eta) + 4H_{-1,-1,1,0}(\eta) \\
&\qquad + 12H_{-1,0,0,-1}(\eta) - 8H_{-1,0,0,0}(\eta) - 12H_{-1,0,0,1}(\eta) + 4H_{-1,1,-1,0}(\eta) \\
&\qquad + 4H_{-1,1,0,-1}(\eta) - 4H_{-1,1,0,0}(\eta) - 4H_{-1,1,0,1}(\eta) - 4H_{0,-1,-1,0}(\eta) \\
&\qquad + 8H_{0,-1,0,-1}(\eta) - 8H_{0,-1,0,1}(\eta) - 4H_{0,-1,1,0}(\eta) + 8H_{0,0,-1,0}(\eta) \\
&\qquad - 24H_{0,0,0,-1}(\eta) + 24H_{0,0,0,1}(\eta) - 8H_{0,0,1,0}(\eta) - 4H_{0,1,-1,0}(\eta) \\
&\qquad - 8H_{0,1,0,-1}(\eta) + 8H_{0,1,0,1}(\eta) - 4H_{0,1,1,0}(\eta) + 4H_{1,-1,0,-1}(\eta) \\
&\qquad - 4H_{1,-1,0,0}(\eta) - 4H_{1,-1,0,1}(\eta) - 4H_{1,-1,1,0}(\eta) - 12H_{1,0,0,-1}(\eta) \\
&\qquad + 8H_{1,0,0,0}(\eta) + 12H_{1,0,0,1}(\eta) - 4H_{1,1,-1,0}(\eta) - 4H_{1,1,0,-1}(\eta) \\
&\qquad + 4H_{1,1,0,0}(\eta) + 4H_{1,1,0,1}(\eta).
\end{aligned} \tag{4.3}$$

To compute the discontinuity in u_2 at $u_2 = 0$, we use the fact that $u_2 \approx 2(1-\eta)$ in this limit. We take the discontinuity in eq. (4.3) at $\eta = 1$ by clipping the index "1" off the back of the HPL index list, and obtain:

$$\begin{aligned}
\text{disc}_{u_2}\left[\mathcal{R}_4^{(2)}(\eta)|_{\text{finite part}}\right] = \pm i\pi\Big[&4H_{-1,-1,0}(\eta) - 12H_{-1,0,0}(\eta) - 4H_{-1,1,0}(\eta) - 8H_{0,-1,0}(\eta) \\
&+ 24H_{0,0,0}(\eta) + 8H_{0,1,0}(\eta) - 4H_{1,-1,0}(\eta) + 12H_{1,0,0}(\eta) + 4H_{1,1,0}(\eta)\Big].
\end{aligned} \tag{4.4}$$

As we return to the OPE limit point, $\eta \to 0$, the discontinuity behaves like,

$$\text{disc}_{u_2}\left[\mathcal{R}_4^{(2)}(\eta)|_{\text{finite part}}\right] \to \pm 4\pi i \ln^3 \eta\,, \tag{4.5}$$

i.e. ζ_3 does not appear. Hence there is no $\ln u_2 \otimes \zeta_3$ term in the $\{1,3\}$ coproduct of $\mathcal{R}_4^{(2)}$ at this point.

To reveal possible terms of the form $\ln v_1 \otimes \zeta_3$ and $\ln v_2 \otimes \zeta_3$, we need to take the two-segment paths $\mathscr{P}\mathscr{Q}_i$ shown in Fig. 4. From the OPE limit point $(u_1, u_2, u_3, v_1, v_2) = (0, 1, 0, 1, 1)$, we first use the same path $\mathscr{P}$, where u_2 varies, to reach the limit $(u_1, u_2, u_3, v_1, v_2) = (0, 0, 0, 1, 1)$. This portion is shown in blue in Fig. 4. Then we vary either v_1 or v_2 to connect to either $(u_1, u_2, u_3, v_1, v_2) = (0, 0, 0, 1, 0)$ or $(u_1, u_2, u_3, v_1, v_2) = (0, 0, 0, 0, 1)$ via the segments $\mathscr{Q}_1$ (green) or $\mathscr{Q}_2$ red, respectively, in Fig. 4. The v_1 and v_2 discontinuities appear at the endpoints of these segments.

The symbol alphabet on the $u_1, u_2, u_3 \to 0$, $0 < v_1, v_2 < 1$ surface, which contains the green and red segments, simplifies to $\{v_1, v_2, 1 - v_1, 1 - v_2, 1 - v_1 - v_2, v_1 + v_2\}$. The finite part of the remainder function can be represented on this surface in terms of G-functions, as shown in Appendix C. Near $v_2 \to 1$, the expression becomes simple logarithms,

$$\begin{aligned}\mathcal{R}^{(2)}_{4,\text{finite}}|_{u_i\to 0, v_2\to 1} = &\frac{1}{8}\ln^4(1-v_1) - \frac{1}{2}\ln^3(1-v_1)\ln v_1 + \frac{3}{4}\ln^2(1-v_1)\ln^2 v_1 \\ &- \frac{1}{2}\ln(1-v_1)\ln^3 v_1 + \frac{1}{8}\ln^4 v_1 - \frac{1}{4}\ln^2(1-v_1)\ln^2(1-v_2) \\ &+ \frac{1}{2}\ln(1-v_1)\ln v_1 \ln^2(1-v_2) - \frac{1}{4}\ln^2 v_1 \ln^2(1-v_2) + \frac{1}{8}\ln^4(1-v_2).\end{aligned} \tag{4.6}$$

Then, when we cycle around $v_1 = 0$, by letting $\ln v_1 \to \ln v_1 \pm i\pi$, and return to the point $(u_2, v_1, v_2) = (0, 1, 1)$ along the red segment $\mathscr{Q}_2$, no ζ_3 appears at $(0, 1, 1)$. Furthermore, all such discontinuities at $(0, 1, 1)$ either vanish, or else they contain the divergent logarithms $\ln(1 - v_i)$. Because of the overall weight constraint, the latter terms cannot produce a ζ_3 when transported along $\mathscr{P}$. Hence no ζ_3 appears at our base point $(u_2, v_1, v_2) = (1, 1, 1)$. The v_2 discontinuity can be obtained similarly by using the $v_1 \leftrightarrow v_2$ symmetry. Therefore, the $\ln v_1 \otimes \zeta_3$ and $\ln v_2 \otimes \zeta_3$ terms also vanish at the OPE limit point. This concludes our check of antipodal self-duality in $\mathcal{R}_4^{(2)}$ beyond the level of the symbol.

5 Conclusion

In this paper we determined the two-loop four-point form factor of the chiral stress-energy tensor in planar $\mathcal{N} = 4$ SYM [49] in the Euclidean region at function level. We did so by giving the iterated table of coproducts up through weight 4 and explicit G-function representations of the basis functions in boundary kinematics. We made use of the branch cut and dihedral symmetry constraints, as well as several boundary kinematics where the behavior of the remainder function is known. In particular, we made use of a three-parameter rational surface $(u_1 \to 0, u_2 \to v_1 v_2)$, which connects the soft limit, triple collinear limit, 2D kinematics, and OPE limit. The symbol alphabet is rationalized everywhere inside this rational surface. The simplicity on this surface enables us to express the remainder function, as well as the lower weight functions for bulk coproducts, as G-functions with indices that are simple functions of the cross ratios; see for example eq. (3.17).

By imposing the branch cut and symmetry constraints, and matching to known boundary kinematics, we could fix all the zeta values on the rational surface. A similar procedure in general bulk kinematics then gave us the entire table of iterated coproducts at function level, including coproducts necessary for taking derivatives in directions off of the rational surface. The results are presented in the ancillary files. We further evaluated the remainder function in several kinematic regions. Plots illustrating the numerical value of the remainder function on 2D slices of the rational surface are presented in Sec. 4. Also, by carrying the zeta-valued information along various lines, to several other limits in the bulk, we can get all the branch cut discontinuities of the remainder function. Returning to a particular base point, the OPE limit point, after taking such discontinuities, further checks the proposed antipodal self-duality [49] at function level.

With the full function for the two-loop four-point form factor, several further investigations of kinematic regions can be performed. Two such regions are multi-regge kinematics (MRK) and self-crossing kinematics. In MRK, where there is a large rapidity separation between outgoing gluons, the six-gluon remainder function exhibits a factorization after a Fourier-Mellin transformation, both for $2 \to 4$ kinematics [90, 91] and $3 \to 3$ kinematics [92]. This representation has been further exploited to give all-loop order resummations at next-to-next-to-leading logarithmic approximations [93, 94], and soon thereafter to give all subleading logarithmic orders [29]. The four-gluon form factor has a MRK-like region in $2 \to 3$ scattering, where the operator is in the final state, and is emitted centrally between two high-energy final state gluons. The phenomenon of gluon reggeization should be universal [95], even in the presence of this operator, which couples to two gluons. Therefore we expect a similar Fourier-Mellin factorized form for the four-point form factor. The details of such a factorization remain to be studied in detail.

The Wilson loops dual to scattering amplitudes and form factors develop singularities when the Wilson lines intersect. The scattering kinematics are similar to multi-parton scattering in hadronic collisions, but here there are only two incoming gluons, each of which splits into two almost on-shell collinear virtual partons that then scatter off each other [60]. (In the case of the four-point form factor, one pair annihilates into an operator.) For the case of six-gluon scattering, the self-crossing limit is characterized by letting one cross ratio $\hat{u} \to 1$, while the other two cross ratios are set equal to each other, $\hat{w} = \hat{v}$. The four-point form factor self-crossing kinematics constrain three of the five kinematic variables. They are a bit simpler to describe in the OPE variables[2]: $F_2 = 1$, and $T^2 = -S^2(1 + T_2^2 + S_2T_2)/(S_2T_2)$. The logarithmic divergences as one approaches the self-crossing limit can be characterized by a renormalization group equation [96, 97], $\mu\frac{\partial}{\partial\mu}\mathcal{W}_i = -\Gamma^{ij}(\gamma, g)\mathcal{W}_j$, where $\mathcal{W}_1$, $\mathcal{W}_2$ are the framed Wilson loops with crossing and disconnected topology [60], which mix with each other under renormalization. The renormalization scale $\log\mu$ can be chosen as $\log(1 - \hat{u})$ in the six-gluon case. The cross anomalous dimension matrix Γ^{ij} has kinematic dependence only on the local crossing angle γ, and can be determined by comparing with the six-gluon remainder

[2]We thank Benjamin Basso for a discussion on this point.

function [60], or using an all-orders formula based on integrability [12]. For the four-gluon form factor, we also expect a similar evolution of self-crossing singularities, but again the details remain to be investigated.

In conclusion, this paper serves to push forward the study of form factors in planar $\mathcal{N} = 4$ SYM by providing function-level information at two loops and four external legs, results which are complementary to those in ref. [61]. This information, and the methods used, can be utilized further in future studies at higher multiplicity and higher loop orders.

Acknowledgments

We thank Benjamin Basso, Ömer Gürdoğan, Zhengjie Li, Yu-Ting Liu, Andrew Mcleod, Matthias Wilhelm, and Gang Yang for useful discussions. We are grateful to the Simons Center for Geometry and Physics for hospitality during the program "Solving $\mathcal{N} = 4$ super-Yang-Mills theory via Scattering Amplitudes". LD also thanks Humboldt University Berlin for hospitality. This research was supported by the US Department of Energy under contract DE–AC02–76SF00515.

A Remainder function near the OPE limit

In this appendix, we provide the remainder function $\mathcal{R}_4^{(2)}$ in the OPE limit, in a form which can be matched to the FFOPE data. The cross ratios u_i, v_i are expressed in terms of the OPE kinematic variables T, S, T_2, S_2, F_2 using eq. (2.16). We perform a double series expansion in T and T_2 around 0. As mentioned in Sec. 3.2.2, the terms at order T^0 come from the OPE expansion of the MHV six-gluon amplitude and are well-understood and checked to high loop orders. Similarly, the terms at order T_2^0 come from the FFOPE expansion of the three-point form factor, and are also well-understood. Here we focus on terms with positive powers of both T and T_2. The first positive power of T that contributes is T^2. We provide this T^2 term, multiplied by either one or two powers of T_2. At two loops, it has the following form, repeated from eq. (3.22) for convenience:

$$\begin{aligned}\mathcal{R}_4^{(2)} = T^2\Big\{ & T_2(F_2 + F_2^{-1})\Big(\ln T\, A_{1,1} + \ln T_2\, A_{1,2} + A_{1,3} + \zeta_2 A_{1,4}\Big) \\ & + T_2^2\Big[(F_2^2 + F_2^{-2})\Big(\ln T\, A_{2,2,1} + \ln T_2\, A_{2,2,2} + A_{2,2,3} + \zeta_2 A_{2,2,4}\Big) \\ & \qquad + \ln T\, A_{2,0,1} + \ln T_2\, A_{2,0,2} + A_{2,0,3} + \zeta_2 A_{2,0,4}\Big]\Big\} \;+\; \mathcal{O}(T^2 T_2^3)\,.\end{aligned} \tag{A.1}$$

Here the coefficients $A_{1,i}$, $A_{2,2,i}$, and $A_{2,0,i}$, for $i = 1, 2, 3, 4$, depend only on

$$x = S^2, \quad y = S_2^2\,, \tag{A.2}$$

and contain both rational functions in x, y and polylogarithms. At two loops, all the polylogarithms are classical polylogarithms, i.e. Li_n for $n = 2, 3$. The expressions for $A_{1,3}$, $A_{2,2,3}$ and

$A_{2,0,3}$ are quite lengthy, so we provide them instead in an ancillary file, `R42_OPE.txt`, which also contains computer-readable forms of all the other coefficients.

The $A_{1,i}$ coefficients (except $A_{1,3}$) are given by

$$\begin{aligned}
A_{1,1} = \frac{1}{\sqrt{y}}\Big[&4(xy+x+2y+\frac{y}{x})\Big(\mathrm{Li}_2(\frac{x^2}{x^2y+x^2+2xy+y}) + \mathrm{Li}_2(\frac{x}{(1+x)(xy+x+y)}) \\
&+ \mathrm{Li}_2(\frac{-1}{xy+x+y}) - \mathrm{Li}_2(\frac{x}{xy+x+y}) + \mathrm{Li}_2(\frac{-x^2}{y(1+x)^2}) - \mathrm{Li}_2(-\frac{1}{y}) \\
&+ \ln y\big(-2\ln(x^2y+x^2+2xy+y) + \ln(xy+x+y) + \ln(1+y) \\
&+ \ln x + 2\ln(1+x)\ \big) + \frac{3}{2}\ln^2(x^2y+x^2+2xy+y) \\
&- \ln(x^2y+x^2+2xy+y)\big(3\ln(1+x) + \ln(xy+x+y) + \ln x\big) \\
&+ \frac{1}{2}\ln^2(xy+x+y) + \ln(xy+x+y)\big(\ln(1+x) - \ln(1+y)\big) + \frac{5}{2}\ln^2(1+x)\Big) \\
&+ \frac{4y(1+x)^2}{x}\ln(1+x)\Big(2\ln x - 2\ln(1+x) + 3\Big) \\
&- 8(xy+x+2y+\frac{y}{x})\ln(x^2y+x^2+2xy+y) + 12x\ln x + 4x(y+1)\ln(1+y) \\
&+ \frac{4y(2xy+2x+y+2)}{x(y+1)}\ln y + \frac{4(xy+x+y)^2}{x(y+1)}\ln(xy+x+y)\Big],
\end{aligned} \tag{A.3}$$

$$\begin{aligned}
A_{1,2} = \frac{1}{\sqrt{y}}\Big[&2(xy+x+2y+\frac{y}{x})\Big(\mathrm{Li}_2(\frac{x^2}{x^2y+x^2+2xy+y}) + \mathrm{Li}_2(\frac{-x^2}{y(1+x)^2}) \\
&+ \big(\ln y + 2\ln(1+x)\big)\big(\frac{1}{2}\ln y + 2\ln x + \ln(1+x) - 2\ln(x^2y+x^2+2xy+y)\big) \\
&- 2\ln x\ln(x^2y+x^2+2xy+y) + \frac{3}{2}\ln^2(x^2y+x^2+2xy+y)\Big) \\
&+ 2(xy+x+2y)\big(\ln y\ln(1+y) - \ln^2(1+y)\big) \\
&- 4(xy+x+2y+\frac{y}{x})\ln(x^2y+x^2+2xy+y) + 8x\ln x \\
&+ 8\frac{y(1+x)^2}{x}\ln(1+x) + 4y(1+\frac{1}{x})\ln y + 4(1+x)(1+y)\ln(1+y)\Big],
\end{aligned} \tag{A.4}$$

$$\begin{aligned}
A_{1,4} = \frac{1}{\sqrt{y}}\Big[&2(2xy+2x+4y+3\frac{y}{x})\ln y + 4(3xy+x+6y+3\frac{y}{x})\ln(1+x) \\
&+ 2(xy+x+2y)\ln(1+y) - 6(xy+x+2y+\frac{y}{x})\ln(x^2y+x^2+2xy+y) \\
&- 4 + 4x\Big].
\end{aligned} \tag{A.5}$$

The coefficients $A_{2,2,i}$ (except $A_{2,2,3}$) are given by

$$
\begin{aligned}
A_{2,2,1} = &- 4\frac{(1+x)^2 y}{x}\Big(\mathrm{Li}_2(\frac{x^2}{x^2y+x^2+2xy+y}) + \mathrm{Li}_2(\frac{x}{(1+x)(xy+x+y)}) \\
&+ \mathrm{Li}_2(\frac{-1}{xy+x+y}) - \mathrm{Li}_2(\frac{x}{xy+x+y}) + \mathrm{Li}_2(\frac{-x^2}{y(1+x)^2}) - \mathrm{Li}_2(\frac{-1}{y}) \\
&+ \ln y(-2\ln(x^2y+x^2+2xy+y) + \ln(xy+x+y) + \ln(1+y) + \ln x + 2\ln(1+x)) \\
&+ \frac{3}{2}\ln^2(x^2y+x^2+2xy+y) - (3\ln(1+x) + \ln(xy+x+y) + \ln x)\ln(x^2y+x^2+2xy+y) \\
&+ \frac{1}{2}\ln^2(xy+x+y) + (\ln(1+x) - \ln(1+y))\ln(xy+x+y) \\
&+ \frac{1}{2}\ln(1+x)(\ln(1+x) + 4\ln x)\Big) \\
&- 4x\ln x - 4xy\ln(1+y) - 8\frac{y(1+x)^2}{x}\ln(1+x) - 4\frac{y(2xy^2+2xy+y^2+1+y)}{x(1+y)^2}\ln y \\
&- 4\frac{(xy+x+y)^2}{x(1+y)^2}\ln(xy+x+y) \\
&+ 4(xy+x+2y+\frac{y}{x})\ln(x^2y+x^2+2xy+y) + 4\frac{y}{1+y}\,,
\end{aligned}
\tag{A.6}
$$

$$
\begin{aligned}
A_{2,2,2} = &- 2\frac{y(1+x)^2}{x}\Big(\mathrm{Li}_2(\frac{x^2}{x^2y+x^2+2xy+y}) + \mathrm{Li}_2(\frac{-x^2}{y(1+x)^2}) \\
&+ 2(\frac{1}{2}\ln y + \ln(1+x))(\frac{1}{2}\ln y + 2\ln x + \ln(1+x) - 2\ln(x^2y+x^2+2xy+y)) \\
&- 2\ln x\ln(x^2y+x^2+2xy+y) + \frac{3}{2}\ln^2(x^2y+x^2+2xy+y)\Big) \\
&- 2y(2+x)(\ln y - \ln(1+y))\ln(1+y) - 2\frac{(2x^2y-x^2+4xy+2y)x}{(1+x)^2y}\ln x \\
&- 6\frac{y(1+x)^2}{x}\ln(1+x) - \frac{(4xy+3y+3)y}{x(1+y)}\ln y \\
&- \frac{3xy^3+5xy^2+2y^3+xy+10y^2-x+2y+2}{y(1+y)}\ln(1+y) \\
&+ \frac{(x^2y+x^2+2xy+y)(3x^2y-x^2+6xy+3y)}{(1+x)^2xy}\ln(x^2y+x^2+2xy+y) + 2\,,
\end{aligned}
\tag{A.7}
$$

$$
\begin{aligned}
A_{2,2,4} = &- 2y(2x+4+\frac{3}{x})\ln y - 12\frac{y(1+x)^2}{x}\ln(1+x) \\
&- 2y(2+x)\ln(1+y) + 6\frac{y(1+x)^2}{x}\ln(x^2y+x^2+2xy+y) \\
&- 4x + \frac{3x+2}{y(1+x)^2} + \frac{4y}{y+1}\,.
\end{aligned}
\tag{A.8}
$$

Finally, the coefficients $A_{2,0,i}$ (except $A_{2,0,3}$) are given by

$$
\begin{aligned}
A_{2,0,1} = &-8\frac{(1+x)^2 y}{x}\Big(\mathrm{Li}_2(\frac{x^2}{x^2y+x^2+2xy+y}) + \mathrm{Li}_2(\frac{x}{(1+x)(xy+x+y)}) + \mathrm{Li}_2(\frac{-1}{xy+x+y}) \\
&\quad - \mathrm{Li}_2(\frac{-x}{y(1+x)}) - 2\mathrm{Li}_2(\frac{x}{xy+x+y}) + \mathrm{Li}_2(\frac{-x^2}{y(1+x)^2}) - \mathrm{Li}_2(\frac{-1}{y}) + \frac{3}{2}\ln^2(x^2y+x^2+2xy+y) \\
&\quad - \ln^2(xy+x+y) + \frac{3}{4}\ln^2(1+x) - \ln y\big(\frac{1}{2}\ln y - 2\ln(xy+x+y)\big) \\
&\quad - (\ln y - \ln(xy+x+y))(\ln x + \ln(1+x) + \ln(1+y)) + \frac{1}{4}\ln(1+x)(\ln(1+x) + 4\ln x) \\
&\quad + \ln y\big(-2\ln(x^2y+x^2+2xy+y) + \ln(xy+x+y) + \ln(1+y) + \ln x + 2\ln(1+x)\big) \\
&\quad - (3\ln(1+x) + \ln(xy+x+y) + \ln x)\ln(x^2y+x^2+2xy+y) + \ln(\frac{1+x}{1+y})\ln(xy+x+y)\Big) \\
&+ 8\frac{x}{y}\Big(\mathrm{Li}_2(\frac{x}{xy+x+y}) + \mathrm{Li}_2(\frac{-x}{y(1+x)}) + \big(\ln y - \ln(xy+x+y)\big)\big(\ln x + \ln(1+x) + \ln(1+y)\big) \\
&\quad + \ln y\big(\frac{1}{2}\ln y - 2\ln(xy+x+y)\big) + \frac{1}{2}\ln^2(1+x) + \frac{3}{2}\ln^2(xy+x+y)\Big) \\
&+ 16(1+x)\Big(\mathrm{Li}_2(\frac{x}{xy+x+y}) + \mathrm{Li}_2(\frac{-x}{y(1+x)}) + \frac{3}{2}\ln^2(xy+x+y) - \frac{3}{4}\ln^2(1+x) \\
&\quad + \ln y\big(\frac{1}{2}\ln y - 2\ln(xy+x+y)\big) + \frac{1}{4}\ln(1+x)\big(\ln(1+x) + 4\ln x\big) \\
&\quad + \big(\ln y - \ln(xy+x+y)\big)\big(\ln x + \ln(1+x) + \ln(1+y)\big)\Big) \\
&+ 8(1+\frac{x}{y})\ln x - 8\frac{(y-1)(1+x)^2}{x}\ln(1+x) - 8\frac{xy^3 - xy^2 - 3xy - y^2 - x}{x(1+y)^2}\ln y \\
&+ 8(2x+y+1+\frac{x}{y})\ln(1+y) - 8\frac{(y^2+3y+1)(xy+x+y)^2}{xy(1+y)^2}\ln(xy+x+y) \\
&+ 8(xy+x+2y+\frac{y}{x})\ln(x^2y+x^2+2xy+y) + 8\frac{y}{1+y}\,,
\end{aligned}
\tag{A.9}
$$

$$
\begin{aligned}
A_{2,0,2} =& 4\frac{(xy+x+y)^2}{xy}\Big(\mathrm{Li}_2(\frac{-x}{x^2y+x^2+2xy+y}) + 2\mathrm{Li}_2(\frac{x}{xy+x+y}) \\
&- \mathrm{Li}_2(\frac{-1}{xy+x+y}) + \mathrm{Li}_2(\frac{-x}{y(1+x)}) + \mathrm{Li}_2(\frac{-1}{y}) \\
&+ (2\ln x - \ln(xy+x+y) - \ln(x^2y+x^2+2xy+y))\ln(1+x) \\
&+ \ln y(2\ln x + \ln y + \ln(1+x) + \ln(1+y) - 3\ln(xy+x+y)) \\
&- \ln(xy+x+y)(2\ln x + \ln(x^2y+x^2+2xy+y)) \\
&+ \frac{1}{2}\ln^2(x^2y+x^2+2xy+y) - \ln^2(1+y) \\
&+ \frac{1}{2}\ln^2(1+x) + \frac{5}{2}\ln^2(xy+x+y)\Big) \\
&- 4\frac{(1+x)^2y}{x}\Big(\mathrm{Li}_2(\frac{x^2}{x^2y+x^2+2xy+y}) + \mathrm{Li}_2(\frac{-x^2}{y(1+x)^2}) \\
&+ (\ln y + 2\ln(1+x))(\frac{1}{2}\ln y + 2\ln x + \ln(1+x) - 2\ln(x^2y+x^2+2xy+y)) \\
&- 2\ln x\ln(x^2y+x^2+2xy+y) + \ln y\ln(1+y) \\
&- \ln^2(1+y) + \frac{3}{2}\ln^2(x^2y+x^2+2xy+y)\Big) \\
&+ 8\frac{x^3+x^2y+x^2+2xy+x+y}{y(1+x)^2}\ln x - 8\frac{y(1+x)^2}{x}\ln(1+x) \\
&- 4\frac{y^2-2y-1}{1+y}\ln y + 4\frac{2xy^2+y^3+4xy+2x+3y}{y(1+y)}\ln(1+y) \\
&- 8\frac{(xy+x+y)^2}{xy}\ln(xy+x+y) \\
&+ \frac{4(x^2y+x^2+2xy+y)(2x^2y+4xy+x+2y)}{(1+x)^2xy}\ln(x^2y+x^2+2xy+y) + 8\,,
\end{aligned}
\tag{A.10}
$$

$$
\begin{aligned}
A_{2,0,4} =& -4\frac{3x^2y^2-6x^2y+6xy^2-x^2-6xy+3y^2}{xy}\ln(1+x) \\
&- 12\frac{(xy+x+y)^2}{xy}\ln(xy+x+y) + 4\frac{2xy+x+2y}{y}(2\ln y + \ln(1+y)) \\
&+ 12\frac{y(1+x)^2}{x}\ln(x^2y+x^2+2xy+y) - 4\frac{x^2}{y(1+x)^2} + 4\frac{3y+1}{y+1}\,.
\end{aligned}
\tag{A.11}
$$

B Remainder function in 2D kinematics

When the external momenta all lie in the same 2D plane, the remainder function reduces to G-functions of v_1, v_2:

$$
\begin{aligned}
\mathcal{R}_4^{(2)} &= -16\zeta_4 + 12\zeta_3\Big[G_0(v_1) + G_1(v_1) + G_0(v_2) + G_1(v_2)\Big] \\
&+ 4\zeta_2\Big[G_0^2(v_1) + G_0(v_1)G_0(v_2) + G_1(v_1)G_0(v_2) + 2G_1(v_1)G_1(v_2) + 4G_0(v_1)G_1(v_2) + 3G_1(v_2)G_0(v_2) \\
&\qquad - 2G_0(v_1)G_0(v_1-v_2) + G_0^2(v_1-v_2) - 2G_{0,1}(1-v_2) - 2G_{0,1}\Big(\frac{-v_2}{v_1-v_2}\Big) - 2G_{-v_1+v_2,-1+v_2}(v_2)\Big] \\
&+ 2G_0^3(1-v_1)G_0(v_1) - 2G_1(v_1)G_0^3(v_1) - 8G_1(v_1)G_0^2(v_1)G_1(v_2) - 4G_0^2(1-v_1)G_0(v_1)G_1(v_1+v_2) \\
&+ 2G_1(v_1)G_0(v_1)G_1^2(v_1+v_2) + 4G_1(v_1)G_0^2(v_1)G_0(v_1-v_2) - 2G_1(v_1)G_0(v_1)G_0^2(v_1-v_2) \\
&+ 2G_0^2(1-v_1)G_0(v_1)G_0(v_2) + 2G_1(v_1)G_0^2(v_1)G_0(v_2) - 8G_1(v_1)G_0(v_1)G_1(v_2)G_0(v_2) \\
&- 4G_1(v_1)G_0(v_1)G_1(v_1+v_2)G_0(v_2) + 2G_0(v_1)G_1^2(v_1+v_2)G_0(v_2) - 4G_1(v_1)G_0(v_1)G_0(v_1-v_2)G_0(v_2) \\
&+ 2G_1(v_1)G_0^2(v_1-v_2)G_0(v_2) - 4G_1(v_1)G_1(v_2)G_0^2(v_2) - 4G_0(v_1)G_1(v_2)G_0^2(v_2) \\
&- 6G_1^2(v_2)G_0^2(v_2) - 4G_0^2(1-v_1)G_{0,1}(1-v_1) + 4G_0^2(v_1)G_{0,1}(1-v_1) \\
&- 8G_1(v_1)G_1(v_2)G_{0,1}(1-v_1) + 8G_0(v_1)G_1(v_2)G_{0,1}(1-v_1) + 8G_1(v_1)G_1(v_1+v_2)G_{0,1}(1-v_1) \\
&- 4G_1^2(v_1+v_2)G_{0,1}(1-v_1) - 8G_0(v_1)G_0(v_1-v_2)G_{0,1}(1-v_1) + 4G_0^2(v_1-v_2)G_{0,1}(1-v_1) \\
&- 4G_1(v_1)G_1(v_2)G_{0,1}(1-v_2) - 4G_0(v_1)G_1(v_2)G_{0,1}(1-v_2) + 4G_1(v_1)G_0(v_2)G_{0,1}(1-v_2) \\
&+ 4G_0(v_1)G_0(v_2)G_{0,1}(1-v_2) + 8G_1(v_2)G_0(v_2)G_{0,1}(1-v_2) - 8G_{0,1}^2(1-v_2) \\
&+ 4\Big[G_1(v_1)\Big(G_0(v_1) - G_0(v_2)\Big) - 2G_{0,1}(1-v_1)\Big]\Big[G_{0,1}\Big(\frac{-v_2}{v_1-v_2}\Big) - G_{0,1}\Big(\frac{-v_2}{1-v_1-v_2}\Big)\Big] \\
&+ 4G_1(v_1)\Big(G_0(v_1) - G_0(v_2)\Big)G_{-v_1+v_2,-1+v_2}(v_2) - 8G_{0,1}(1-v_1)G_{-v_1+v_2,-1+v_2}(v_2) \\
&- 4G_0(v_1)\Big(G_1(v_1) + G_0(v_2)\Big)G_{-1+v_1+v_2,-1+v_2}(v_2) + 8G_{0,1}(1-v_1)G_{-1+v_1+v_2,-1+v_2}(v_2) \\
&+ 24G_1(v_2)\Big(G_{0,0,1}(1-v_1) + G_{0,0,1}(v_1)\Big) + 12\Big(G_0(v_1) + G_1(v_1) + G_0(v_2)\Big)G_{0,0,1}(1-v_2) \\
&+ 4G_1(v_2)G_{0,0,1}(1-v_2) + 12\Big(G_0(v_1) + G_1(v_1) + G_1(v_2)\Big)G_{0,0,1}(v_2) + 4G_0(v_2)G_{0,0,1}(v_2) \\
&- 8G_0(v_1)G_{0,0,1}\Big(\frac{v_2}{1-v_1}\Big) - 8G_1(v_1)G_{0,0,1}\Big(\frac{v_2}{v_1}\Big) - 4G_1(v_1)\Big(G_{-v_1+v_2,-1+v_2,v_2}(v_2) + G_{-v_1+v_2,v_2,-1+v_2}(v_2)\Big) \\
&+ 4\Big(G_0(v_1) + G_0(v_2)\Big)\Big(G_{-1+v_2,-v_1+v_2,v_2}(v_2) - G_{-1+v_2,-v_1+v_2,-1+v_2}(v_2)\Big) \\
&+ 4\Big(G_1(v_1) + G_0(v_2)\Big)\Big(G_{-1+v_2,-1+v_1+v_2,v_2}(v_2) - G_{-1+v_2,-1+v_1+v_2,-1+v_2}(v_2)\Big) \\
&- 4G_0(v_1)G_{-1+v_1+v_2,-1+v_2,v_2}(v_2) - 4G_0(v_1)G_{-1+v_1+v_2,v_2,-1+v_2}(v_2) - 16G_{0,0,0,1}(1-v_2) - 16G_{0,0,0,1}(v_2) \\
&- 8G_{-1+v_2,v_2,-v_1+v_2,-1+v_2}(v_2) + 8G_{-1+v_2,v_2,-v_1+v_2,v_2}(v_2) - 8G_{-1+v_2,v_2,-1+v_1+v_2,-1+v_2}(v_2) \\
&+ 8G_{-1+v_2,v_2,-1+v_1+v_2,v_2}(v_2) - 4G_{-1+v_2,-v_1+v_2,-1+v_2,v_2}(v_2) - 4G_{-1+v_2,-v_1+v_2,v_2,-1+v_2}(v_2) \\
&+ 8G_{-1+v_2,-v_1+v_2,v_2,v_2}(v_2) - 4G_{-1+v_2,-1+v_1+v_2,-1+v_2,v_2}(v_2) - 4G_{-1+v_2,-1+v_1+v_2,v_2,-1+v_2}(v_2) \\
&+ 8G_{-1+v_2,-1+v_1+v_2,v_2,v_2}(v_2)\,.
\end{aligned}
\tag{B.1}
$$

C Remainder function near $u_1, u_2, u_3 \to 0$

In order to connect the point $(u_1, u_2, u_3, v_1, v_2) = (0, 0, 0, 1, 1)$ to either $(0, 0, 0, 0, 1)$ or $(0, 0, 0, 1, 0)$, we integrated up the remainder function on the surface where $u_1, u_2, u_3 \to 0$, and $0 < v_1, v_2 < 1$. For convenience, we took the limit with $u_1 \ll u_3 \ll u_2$ (the precise hierarchy between the u_i may not matter). In this limit, the singular variable u_2 drops out, and the remainder function has only a mild logarithmic divergence involving $\ln u_1$ and $\ln u_3$:

$$R_4^{(2)}|_{u_i \to 0} = R^{(2)}_{4,\text{finite}} + \ln u_1 R^{(2)}_{4,\text{div1}} + \ln u_3 R^{(2)}_{4,\text{div2}} + \ln u_1 \ln u_3 R^{(2)}_{4,\text{div3}} \,. \tag{C.1}$$

The finite part is:

$$\begin{aligned}
R^{(2)}_{4,\text{finite}} = &- G_{0,0}(1-v_1)G_{0,0}(1-v_2) + G_{0,0}(1-v_2)G_{0,1}(1-v_1) + G_{0,0}(1-v_1)G_{0,1}(1-v_2) \\
&- G_{0,1}(1-v_1)G_{0,1}(1-v_2) + G_{0,0}(1-v_2)G_{1,0}(1-v_1) - G_{0,1}(1-v_2)G_{1,0}(1-v_1) \\
&- G_{0,0}(1-v_2)G_{1,1}(1-v_1) + G_{0,1}(1-v_2)G_{1,1}(1-v_1) - 2G_{0,0}(1-v_1)G_{1,1}(1-v_2) \\
&+ 2G_{0,1}(1-v_1)G_{1,1}(1-v_2) + 2G_{1,0}(1-v_1)G_{1,1}(1-v_2) - 2G_{1,1}(1-v_1)G_{1,1}(1-v_2) \\
&+ 2G_{0,0}(1-v_1)G_{1,v_1}(1-v_2) - 2G_{0,1}(1-v_1)G_{1,v_1}(1-v_2) - 2G_{1,0}(1-v_1)G_{1,v_1}(1-v_2) \\
&+ 2G_{1,1}(1-v_1)G_{1,v_1}(1-v_2) + G_{0,0}(1-v_1)G_{v_1,0}(1-v_2) - G_{0,1}(1-v_1)G_{v_1,0}(1-v_2) \\
&- G_{1,0}(1-v_1)G_{v_1,0}(1-v_2) + G_{1,1}(1-v_1)G_{v_1,0}(1-v_2) + G_{0,0}(1-v_1)G_{v_1,1}(1-v_2) \\
&- G_{0,1}(1-v_1)G_{v_1,1}(1-v_2) - G_{1,0}(1-v_1)G_{v_1,1}(1-v_2) + G_{1,1}(1-v_1)G_{v_1,1}(1-v_2) \\
&- 2G_{0,0}(1-v_1)G_{v_1,v_1}(1-v_2) + 2G_{0,1}(1-v_1)G_{v_1,v_1}(1-v_2) + 2G_{1,0}(1-v_1)G_{v_1,v_1}(1-v_2) \\
&- 2G_{1,1}(1-v_1)G_{v_1,v_1}(1-v_2) - G_1(1-v_2)G_{0,0,0}(1-v_1) + G_{v_1}(1-v_2)G_{0,0,0}(1-v_1) \\
&+ G_1(1-v_2)G_{0,0,1}(1-v_1) - G_{v_1}(1-v_2)G_{0,0,1}(1-v_1) - G_0(1-v_1)G_{0,0,1}(1-v_2) \\
&+ G_1(1-v_1)G_{0,0,1}(1-v_2) + G_0(1-v_1)G_{0,0,v_1}(1-v_2) - G_1(1-v_1)G_{0,0,v_1}(1-v_2) \\
&+ G_1(1-v_2)G_{0,1,0}(1-v_1) - G_{v_1}(1-v_2)G_{0,1,0}(1-v_1) - G_0(1-v_1)G_{0,1,0}(1-v_2) \\
&+ G_1(1-v_1)G_{0,1,0}(1-v_2) - G_1(1-v_2)G_{0,1,1}(1-v_1) + G_{v_1}(1-v_2)G_{0,1,1}(1-v_1) \\
&+ 2G_0(1-v_1)G_{0,1,1}(1-v_2) - 2G_1(1-v_1)G_{0,1,1}(1-v_2) - G_0(1-v_1)G_{0,1,v_1}(1-v_2) \\
&+ G_1(1-v_1)G_{0,1,v_1}(1-v_2) + G_0(1-v_1)G_{0,v_1,0}(1-v_2) - G_1(1-v_1)G_{0,v_1,0}(1-v_2) \\
&- G_0(1-v_1)G_{0,v_1,1}(1-v_2) + G_1(1-v_1)G_{0,v_1,1}(1-v_2) + G_1(1-v_2)G_{1,0,0}(1-v_1) \\
&- G_{v_1}(1-v_2)G_{1,0,0}(1-v_1) - G_0(1-v_1)G_{1,0,0}(1-v_2) + G_1(1-v_1)G_{1,0,0}(1-v_2) \\
&- G_1(1-v_2)G_{1,0,1}(1-v_1) + G_{v_1}(1-v_2)G_{1,0,1}(1-v_1) + G_0(1-v_1)G_{1,0,1}(1-v_2) \\
&- G_1(1-v_1)G_{1,0,1}(1-v_2) - G_1(1-v_2)G_{1,1,0}(1-v_1) + G_{v_1}(1-v_2)G_{1,1,0}(1-v_1) \\
&+ G_1(1-v_2)G_{1,1,1}(1-v_1) - G_{v_1}(1-v_2)G_{1,1,1}(1-v_1) + G_0(1-v_1)G_{1,v_1,0}(1-v_2) \\
&- G_1(1-v_1)G_{1,v_1,0}(1-v_2) - G_0(1-v_1)G_{1,v_1,1}(1-v_2) + G_1(1-v_1)G_{1,v_1,1}(1-v_2) \\
&+ G_0(1-v_1)G_{v_1,0,0}(1-v_2) - G_1(1-v_1)G_{v_1,0,0}(1-v_2) - G_0(1-v_1)G_{v_1,0,v_1}(1-v_2) \\
&+ G_1(1-v_1)G_{v_1,0,v_1}(1-v_2) + G_0(1-v_1)G_{v_1,1,0}(1-v_2) - G_1(1-v_1)G_{v_1,1,0}(1-v_2) \\
&- 2G_0(1-v_1)G_{v_1,1,1}(1-v_2) + 2G_1(1-v_1)G_{v_1,1,1}(1-v_2) + G_0(1-v_1)G_{v_1,1,v_1}(1-v_2)
\end{aligned}$$

$$
\begin{aligned}
&- G_1(1-v_1)G_{v_1,1,v_1}(1-v_2) - 2G_0(1-v_1)G_{v_1,v_1,0}(1-v_2) + 2G_1(1-v_1)G_{v_1,v_1,0}(1-v_2) \\
&+ 2G_0(1-v_1)G_{v_1,v_1,1}(1-v_2) - 2G_1(1-v_1)G_{v_1,v_1,1}(1-v_2) + 3G_{0,0,0,0}(1-v_1) \\
&+ 3G_{0,0,0,0}(1-v_2) - 3G_{0,0,0,1}(1-v_1) - G_{0,0,0,1}(1-v_2) - 2G_{0,0,0,v_1}(1-v_2) \\
&- 3G_{0,0,1,0}(1-v_1) - 2G_{0,0,1,0}(1-v_2) + 3G_{0,0,1,1}(1-v_1) + 2G_{0,0,1,v_1}(1-v_2) \\
&- G_{0,0,v_1,0}(1-v_2) + G_{0,0,v_1,1}(1-v_2) - 3G_{0,1,0,0}(1-v_1) \\
&- 3G_{0,1,0,0}(1-v_2) + 3G_{0,1,0,1}(1-v_1) + G_{0,1,0,1}(1-v_2) \\
&+ 2G_{0,1,0,v_1}(1-v_2) + 3G_{0,1,1,0}(1-v_1) + 2G_{0,1,1,0}(1-v_2) - 3G_{0,1,1,1}(1-v_1) \\
&- 2G_{0,1,1,v_1}(1-v_2) + G_{0,1,v_1,0}(1-v_2) - G_{0,1,v_1,1}(1-v_2) \\
&- 3G_{1,0,0,0}(1-v_1) - 4G_{1,0,0,0}(1-v_2) + 3G_{1,0,0,1}(1-v_1) + 2G_{1,0,0,1}(1-v_2) \\
&+ 2G_{1,0,0,v_1}(1-v_2) + 3G_{1,0,1,0}(1-v_1) + 2G_{1,0,1,0}(1-v_2) - 3G_{1,0,1,1}(1-v_1) \\
&- 2G_{1,0,1,v_1}(1-v_2) + 2G_{1,0,v_1,0}(1-v_2) - 2G_{1,0,v_1,1}(1-v_2) + 3G_{1,1,0,0}(1-v_1) \\
&+ 2G_{1,1,0,0}(1-v_2) - 3G_{1,1,0,1}(1-v_1) - 2G_{1,1,0,1}(1-v_2) - 3G_{1,1,1,0}(1-v_1) \\
&+ 3G_{1,1,1,1}(1-v_1) - 2G_{1,1,v_1,0}(1-v_2) + 2G_{1,1,v_1,1}(1-v_2) + 2G_{1,v_1,0,0}(1-v_2) \\
&- 2G_{1,v_1,0,v_1}(1-v_2) - 2G_{1,v_1,1,0}(1-v_2) + 2G_{1,v_1,1,v_1}(1-v_2) + G_{v_1,0,0,0}(1-v_2) \\
&- G_{v_1,0,0,1}(1-v_2) - G_{v_1,0,v_1,0}(1-v_2) + G_{v_1,0,v_1,1}(1-v_2) \\
&+ G_{v_1,1,0,0}(1-v_2) + G_{v_1,1,0,1}(1-v_2) - 2G_{v_1,1,0,v_1}(1-v_2) - 2G_{v_1,1,1,0}(1-v_2) \\
&+ 2G_{v_1,1,1,v_1}(1-v_2) + G_{v_1,1,v_1,0}(1-v_2) - G_{v_1,1,v_1,1}(1-v_2) - 2G_{v_1,v_1,0,0}(1-v_2) \\
&+ 2G_{v_1,v_1,0,v_1}(1-v_2) + 2G_{v_1,v_1,1,0}(1-v_2) - 2G_{v_1,v_1,1,v_1}(1-v_2)\,.
\end{aligned}
\tag{C.2}
$$

The divergent parts are

$$
\begin{aligned}
R^{(2)}_{4,\mathrm{div1}} = {} & (G_0(1-v_1) - G_1(1-v_1))G_{0,0}(1-v_2) + (-G_0(1-v_1) + G_1(1-v_1))G_{0,1}(1-v_2) \\
& + G_{v_1}(1-v_2)(-G_{0,0}(1-v_1) + G_{0,1}(1-v_1) + G_{1,0}(1-v_1) - G_{1,1}(1-v_1)) \\
& + G_1(1-v_2)(G_{0,0}(1-v_1) - G_{0,1}(1-v_1) - G_{1,0}(1-v_1) + G_{1,1}(1-v_1)) \\
& + (-G_0(1-v_1) + G_1(1-v_1))G_{v_1,0}(1-v_2) + (G_0(1-v_1) - G_1(1-v_1))G_{v_1,1}(1-v_2) \\
& - G_{0,0,0}(1-v_1) + 2G_{0,0,0}(1-v_2) + G_{0,0,1}(1-v_1) - G_{0,0,1}(1-v_2) \\
& - G_{0,0,v_1}(1-v_2) + G_{0,1,0}(1-v_1) - G_{0,1,0}(1-v_2) - G_{0,1,1}(1-v_1) \\
& + G_{0,1,v_1}(1-v_2) - G_{0,v_1,0}(1-v_2) + G_{0,v_1,1}(1-v_2) + G_{1,0,0}(1-v_1) \\
& - G_{1,0,0}(1-v_2) - G_{1,0,1}(1-v_1) + G_{1,0,1}(1-v_2) - G_{1,1,0}(1-v_1) \\
& + G_{1,1,1}(1-v_1) + G_{1,v_1,0}(1-v_2) - G_{1,v_1,1}(1-v_2) - G_{v_1,0,0}(1-v_2) \\
& + G_{v_1,0,v_1}(1-v_2) + G_{v_1,1,0}(1-v_2) - G_{v_1,1,v_1}(1-v_2)\,,
\end{aligned}
\tag{C.3}
$$

$$
\begin{aligned}
R^{(2)}_{4,\text{div3}} = {} & G_0(1-v_2)(-G_0(1-v_1)+G_1(1-v_1)) + (G_0(1-v_1)-G_1(1-v_1))G_1(1-v_2) \\
& - G_{0,0}(1-v_1) - G_{0,0}(1-v_2) + G_{0,1}(1-v_1) + G_{0,v_1}(1-v_2) \\
& + G_{1,0}(1-v_1) + G_{1,0}(1-v_2) - G_{1,1}(1-v_1) - G_{1,v_1}(1-v_2)\,,
\end{aligned}
\tag{C.4}
$$

and $R^{(2)}_{4,\text{div2}}$ is related to by $R^{(2)}_{4,\text{div2}}$ by the "cycle-then-flip" symmetry (3.8), which exchanges $u_1 \leftrightarrow u_3$, $v_1 \leftrightarrow v_2$:

$$
R^{(2)}_{4,\text{div2}}(v_1, v_2) = R^{(2)}_{4,\text{div1}}(v_2, v_1). \tag{C.5}
$$

The finite part and the $\ln u_1 \ln u_3$ coefficient are both invariant under $v_1 \leftrightarrow v_2$. Thus $R^{(2)}_4|_{u_i \to 0}$ preserves the cycle-then-flip symmetry (3.8).

References

[1] L. J. Dixon, J. M. Drummond and J. M. Henn, *Bootstrapping the three-loop hexagon*, *JHEP* **1111** (2011) 023 [1108.4461].

[2] L. J. Dixon, J. M. Drummond and J. M. Henn, *Analytic result for the two-loop six-point NMHV amplitude in $\mathcal{N} = 4$ super Yang-Mills theory*, *JHEP* **1201** (2012) 024 [1111.1704].

[3] L. J. Dixon, J. M. Drummond, M. von Hippel and J. Pennington, *Hexagon functions and the three-loop remainder function*, *JHEP* **1312** (2013) 049 [1308.2276].

[4] L. J. Dixon, J. M. Drummond, C. Duhr and J. Pennington, *The four-loop remainder function and multi-Regge behavior at NNLLA in planar $\mathcal{N} = 4$ super-Yang-Mills theory*, *JHEP* **1406** (2014) 116 [1402.3300].

[5] L. J. Dixon and M. von Hippel, *Bootstrapping an NMHV amplitude through three loops*, *JHEP* **1410** (2014) 65 [1408.1505].

[6] J. M. Drummond, G. Papathanasiou and M. Spradlin, *A Symbol of Uniqueness: The Cluster Bootstrap for the 3-Loop MHV Heptagon*, *JHEP* **03** (2015) 072 [1412.3763].

[7] L. J. Dixon, M. von Hippel and A. J. McLeod, *The four-loop six-gluon NMHV ratio function*, *JHEP* **01** (2016) 053 [1509.08127].

[8] S. Caron-Huot, L. J. Dixon, A. McLeod and M. von Hippel, *Bootstrapping a Five-Loop Amplitude Using Steinmann Relations*, *Phys. Rev. Lett.* **117** (2016) 241601 [1609.00669].

[9] L. J. Dixon, M. von Hippel, A. J. McLeod and J. Trnka, *Multi-loop positivity of the planar $\mathcal{N} = 4$ SYM six-point amplitude*, *JHEP* **02** (2017) 112 [1611.08325].

[10] L. J. Dixon, J. Drummond, T. Harrington, A. J. McLeod, G. Papathanasiou and M. Spradlin, *Heptagons from the Steinmann Cluster Bootstrap*, *JHEP* **02** (2017) 137 [1612.08976].

[11] J. Drummond, J. Foster, Ö. Gürdoğan and G. Papathanasiou, *Cluster adjacency and the four-loop NMHV heptagon*, *JHEP* **03** (2019) 087 [1812.04640].

[12] S. Caron-Huot, L. J. Dixon, F. Dulat, M. von Hippel, A. J. McLeod and G. Papathanasiou, *Six-Gluon amplitudes in planar $\mathcal{N} = 4$ super-Yang-Mills theory at six and seven loops*, *JHEP* **08** (2019) 016 [1903.10890].

[13] L. J. Dixon, A. J. McLeod and M. Wilhelm, *A Three-Point Form Factor Through Five Loops*, *JHEP* **04** (2021) 147 [2012.12286].

[14] L. J. Dixon, Ö. Gürdoğan, A. J. McLeod and M. Wilhelm, *Bootstrapping a stress-tensor form factor through eight loops*, *JHEP* **07** (2022) 153 [2204.11901].

[15] L. J. Dixon and Y.-T. Liu, *An eight loop amplitude via antipodal duality*, *JHEP* **09** (2023) 098 [2308.08199].

[16] B. Basso, L. J. Dixon and A. G. Tumanov, *The Three-Point Form Factor of $Tr\phi^3$ to Six Loops*, 2410.22402.

[17] B. Basso, A. Sever and P. Vieira, *Spacetime and Flux Tube S-Matrices at Finite Coupling for $\mathcal{N} = 4$ Supersymmetric Yang-Mills Theory*, *Phys. Rev. Lett.* **111** (2013) 091602 [1303.1396].

[18] B. Basso, A. Sever and P. Vieira, *Space-time S-matrix and Flux tube S-matrix II. Extracting and Matching Data*, *JHEP* **1401** (2014) 008 [1306.2058].

[19] B. Basso, A. Sever and P. Vieira, *Space-time S-matrix and Flux-tube S-matrix III. The two-particle contributions*, *JHEP* **08** (2014) 085 [1402.3307].

[20] B. Basso, A. Sever and P. Vieira, *Space-time S-matrix and Flux-tube S-matrix IV. Gluons and Fusion*, *JHEP* **09** (2014) 149 [1407.1736].

[21] B. Basso, J. Caetano, L. Cordova, A. Sever and P. Vieira, *OPE for all Helicity Amplitudes II. Form Factors and Data Analysis*, *JHEP* **12** (2015) 088 [1508.02987].

[22] B. Basso, A. Sever and P. Vieira, *Hexagonal Wilson loops in planar $\mathcal{N} = 4$ SYM theory at finite coupling*, *J. Phys. A* **49** (2016) 41LT01 [1508.03045].

[23] A. Sever, A. G. Tumanov and M. Wilhelm, *Operator Product Expansion for Form Factors*, *Phys. Rev. Lett.* **126** (2021) 031602 [2009.11297].

[24] A. Sever, A. G. Tumanov and M. Wilhelm, *An Operator Product Expansion for Form Factors II. Born level*, *JHEP* **10** (2021) 071 [2105.13367].

[25] A. Sever, A. G. Tumanov and M. Wilhelm, *An Operator Product Expansion for Form Factors III. Finite Coupling and Multi-Particle Contributions*, *JHEP* **03** (2022) 128 [2112.10569].

[26] B. Basso and A. G. Tumanov, *Wilson loop duality and OPE for super form factors of half-BPS operators*, *JHEP* **02** (2024) 022 [2308.08432].

[27] I. I. Balitsky and L. N. Lipatov, *The Pomeranchuk Singularity in Quantum Chromodynamics*, *Sov. J. Nucl. Phys.* **28** (1978) 822.

[28] E. A. Kuraev, L. N. Lipatov and V. S. Fadin, *The Pomeranchuk Singularity in Nonabelian Gauge Theories*, *Sov. Phys. JETP* **45** (1977) 199.

[29] B. Basso, S. Caron-Huot and A. Sever, *Adjoint BFKL at finite coupling: a short-cut from the collinear limit*, *JHEP* **01** (2015) 027 [1407.3766].

[30] V. Del Duca, S. Druc, J. M. Drummond, C. Duhr, F. Dulat, R. Marzucca et al., *All-order amplitudes at any multiplicity in the multi-Regge limit*, *Phys. Rev. Lett.* **124** (2020) 161602 [1912.00188].

[31] L. F. Alday and J. M. Maldacena, *Gluon scattering amplitudes at strong coupling*, *JHEP* **06** (2007) 064 [0705.0303].

[32] J. Drummond, G. Korchemsky and E. Sokatchev, *Conformal properties of four-gluon planar amplitudes and Wilson loops*, *Nucl. Phys. B* **795** (2008) 385 [0707.0243].

[33] A. Brandhuber, P. Heslop and G. Travaglini, *MHV amplitudes in $\mathcal{N} = 4$ super Yang-Mills and Wilson loops*, *Nucl. Phys. B* **794** (2008) 231 [0707.1153].

[34] J. Drummond, J. Henn, G. Korchemsky and E. Sokatchev, *Conformal Ward identities for Wilson loops and a test of the duality with gluon amplitudes*, *Nucl.Phys.* **B826** (2010) 337 [0712.1223].

[35] L. F. Alday and R. Roiban, *Scattering Amplitudes, Wilson Loops and the String/Gauge Theory Correspondence*, *Phys. Rept.* **468** (2008) 153 [0807.1889].

[36] T. Adamo, M. Bullimore, L. Mason and D. Skinner, *Scattering Amplitudes and Wilson Loops in Twistor Space*, *J. Phys. A* **44** (2011) 454008 [1104.2890].

[37] A. Brandhuber, B. Spence, G. Travaglini and G. Yang, *Form Factors in $\mathcal{N} = 4$ Super Yang-Mills and Periodic Wilson Loops*, *JHEP* **01** (2011) 134 [1011.1899].

[38] L. F. Alday and J. Maldacena, *Comments on gluon scattering amplitudes via AdS/CFT*, *JHEP* **0711** (2007) 068 [0710.1060].

[39] Z. Bern, L. J. Dixon, D. A. Kosower, R. Roiban, M. Spradlin, C. Vergu et al., *The Two-Loop Six-Gluon MHV Amplitude in Maximally Supersymmetric Yang-Mills Theory*, *Phys. Rev.* **D78** (2008) 045007 [0803.1465].

[40] J. Drummond, J. Henn, G. Korchemsky and E. Sokatchev, *Hexagon Wilson loop = six-gluon MHV amplitude*, *Nucl.Phys.* **B815** (2009) 142 [0803.1466].

[41] J. Maldacena and A. Zhiboedov, *Form factors at strong coupling via a Y-system*, *JHEP* **11** (2010) 104 [1009.1139].

[42] R. Ben-Israel, A. G. Tumanov and A. Sever, *Scattering amplitudes — Wilson loops duality for the first non-planar correction*, *JHEP* **08** (2018) 122 [1802.09395].

[43] L. Bianchi, A. Brandhuber, R. Panerai and G. Travaglini, *Dual conformal invariance for form factors*, *JHEP* **02** (2019) 134 [1812.10468].

[44] J. M. Drummond, J. Henn, V. A. Smirnov and E. Sokatchev, *Magic identities for conformal four-point integrals*, *JHEP* **01** (2007) 064 [hep-th/0607160].

[45] Z. Bern, M. Czakon, L. J. Dixon, D. A. Kosower and V. A. Smirnov, *The Four-Loop Planar Amplitude and Cusp Anomalous Dimension in Maximally Supersymmetric Yang-Mills Theory*, *Phys. Rev.* **D75** (2007) 085010 [hep-th/0610248].

[46] Z. Bern, J. Carrasco, H. Johansson and D. Kosower, *Maximally supersymmetric planar Yang-Mills amplitudes at five loops*, *Phys.Rev.* **D76** (2007) 125020 [0705.1864].

[47] J. M. Drummond, J. Henn, G. P. Korchemsky and E. Sokatchev, *Dual superconformal symmetry of scattering amplitudes in $\mathcal{N} = 4$ super-Yang-Mills theory*, *Nucl. Phys.* **B828** (2010) 317 [0807.1095].

[48] L. J. Dixon, O. Gürdoğan, A. J. McLeod and M. Wilhelm, *Folding Amplitudes into Form Factors: An Antipodal Duality*, *Phys. Rev. Lett.* **128** (2022) 111602 [2112.06243].

[49] L. J. Dixon, O. Gürdoğan, Y.-T. Liu, A. J. McLeod and M. Wilhelm, *Antipodal Self-Duality for a Four-Particle Form Factor*, *Phys. Rev. Lett.* **130** (2023) 111601 [2212.02410].

[50] L. J. Dixon and Y.-T. Liu, *Lifting Heptagon Symbols to Functions*, *JHEP* **10** (2020) 031 [2007.12966].

[51] Y. Guo, L. Wang and G. Yang, *Analytic Four-Point Lightlike Form Factors and OPE of Null-Wrapped Polygons*, 2209.06816.

[52] Y. Guo, L. Wang and G. Yang, *Bootstrapping a Two-Loop Four-Point Form Factor*, *Phys. Rev. Lett.* **127** (2021) 151602 [2106.01374].

[53] J. M. Henn, J. Lim and W. J. Torres Bobadilla, *Analytic evaluation of the three-loop three-point form factor of* $\mathrm{tr}\,\phi^3$ *in* $\mathcal{N}=4$ *sYM*, 2410.22465.

[54] A. B. Goncharov, M. Spradlin, C. Vergu and A. Volovich, *Classical Polylogarithms for Amplitudes and Wilson Loops*, *Phys. Rev. Lett.* **105** (2010) 151605 [1006.5703].

[55] J. Golden, A. B. Goncharov, M. Spradlin, C. Vergu and A. Volovich, *Motivic Amplitudes and Cluster Coordinates*, *JHEP* **01** (2014) 091 [1305.1617].

[56] L. F. Alday, D. Gaiotto and J. Maldacena, *Thermodynamic Bubble Ansatz*, *JHEP* **09** (2011) 032 [0911.4708].

[57] B. Basso, L. J. Dixon and G. Papathanasiou, *Origin of the Six-Gluon Amplitude in Planar* $N=4$ *Supersymmetric Yang-Mills Theory*, *Phys. Rev. Lett.* **124** (2020) 161603 [2001.05460].

[58] B. Basso, L. J. Dixon, Y.-T. Liu and G. Papathanasiou, *An Origin Story for Amplitudes*, *Phys. Rev. Lett.* **130** (2023) 111602 [2211.12555].

[59] G. Georgiou, *Null Wilson loops with a self-crossing and the Wilson loop/amplitude conjecture*, *JHEP* **09** (2009) 021 [0904.4675].

[60] L. J. Dixon and I. Esterlis, *All orders results for self-crossing Wilson loops mimicking double parton scattering*, *JHEP* **07** (2016) 116 [1602.02107].

[61] Y. Guo, L. Wang, G. Yang and Y. Yin, *Analytic two-Loop four-point form factor of the stress-tensor supermultiplet in* $\mathcal{N}=4$ *SYM*, 2409.12445.

[62] S. Abreu, D. Chicherin, H. Ita, B. Page, V. Sotnikov, W. Tschernow et al., *All Two-Loop Feynman Integrals for Five-Point One-Mass Scattering*, *Phys. Rev. Lett.* **132** (2024) 141601 [2306.15431].

[63] X. Liu and Y.-Q. Ma, *AMFlow: A Mathematica package for Feynman integrals computation via auxiliary mass flow*, *Comput. Phys. Commun.* **283** (2023) 108565 [2201.11669].

[64] N. Beisert, B. Eden and M. Staudacher, *Transcendentality and Crossing*, *J. Stat. Mech.* **0701** (2007) P01021 [hep-th/0610251].

[65] K.-T. Chen, *Iterated path integrals*, *Bull. Amer. Math. Soc.* **83** (1977) 831.

[66] A. Goncharov, *Multiple polylogarithms and mixed Tate motives*, math/0103059.

[67] C. Duhr, H. Gangl and J. R. Rhodes, *From polygons and symbols to polylogarithmic functions*, *JHEP* **10** (2012) 075 [1110.0458].

[68] C. Duhr, *Hopf algebras, coproducts and symbols: an application to Higgs boson amplitudes*, *JHEP* **1208** (2012) 043 [1203.0454].

[69] E. Remiddi and J. Vermaseren, *Harmonic polylogarithms*, *Int. J. Mod. Phys. A* **15** (2000) 725 [hep-ph/9905237].

[70] F. C. Brown, *Multiple zeta values and periods of moduli spaces* $\overline{\mathfrak{M}}_{0,n}(\mathbb{R})$, *Annales Sci.Ecole Norm.Sup.* **42** (2009) 371 [math/0606419].

[71] F. Brown, *Mixed Tate motives over* $\mathbb{Z}$, *Ann. of Math. (2)* **175** (2012) 949 [1102.1312].

[72] F. Brown, *Notes on Motivic Periods*, *Commun. Num. Theor. Phys.* **11** (2017) 557 [1512.06410].

[73] S. Abreu, H. Ita, F. Moriello, B. Page, W. Tschernow and M. Zeng, *Two-Loop Integrals for Planar Five-Point One-Mass Processes*, *JHEP* **11** (2020) 117 [2005.04195].

[74] S. Abreu, H. Ita, B. Page and W. Tschernow, *Two-loop hexa-box integrals for non-planar five-point one-mass processes*, *JHEP* **03** (2022) 182 [2107.14180].

[75] Ö. Gürdoğan. private communication.

[76] S. Caron-Huot, L. J. Dixon, F. Dulat, M. Von Hippel, A. J. McLeod and G. Papathanasiou, *The Cosmic Galois Group and Extended Steinmann Relations for Planar* $\mathcal{N} = 4$ *SYM Amplitudes*, *JHEP* **09** (2019) 061 [1906.07116].

[77] C. Duhr and F. Dulat, *PolyLogTools — polylogs for the masses*, *JHEP* **08** (2019) 135 [1904.07279].

[78] A. Brandhuber, G. Travaglini and G. Yang, *Analytic two-loop form factors in N=4 SYM*, *JHEP* **05** (2012) 082 [1201.4170].

[79] L. F. Alday, D. Gaiotto, J. Maldacena, A. Sever and P. Vieira, *An Operator Product Expansion for Polygonal null Wilson Loops*, *JHEP* **1104** (2011) 088 [1006.2788].

[80] B. Basso, A. Sever and P. Vieira, *Collinear Limit of Scattering Amplitudes at Strong Coupling*, *Phys. Rev. Lett.* **113** (2014) 261604 [1405.6350].

[81] A. Belitsky, *Nonsinglet pentagons and NMHV amplitudes*, *Nucl. Phys. B* **896** (2015) 493 [1407.2853].

[82] A. Belitsky, *Fermionic pentagons and NMHV hexagon*, *Nucl. Phys. B* **894** (2015) 108 [1410.2534].

[83] B. Basso, J. Caetano, L. Cordova, A. Sever and P. Vieira, *OPE for all Helicity Amplitudes*, *JHEP* **08** (2015) 018 [1412.1132].

[84] A. V. Belitsky, *On factorization of multiparticle pentagons*, *Nucl. Phys.* **B897** (2015) 346 [1501.06860].

[85] A. Belitsky, *Matrix pentagons*, *Nucl. Phys. B* **923** (2017) 588 [1607.06555].

[86] M. Wilhelm. private communication.

[87] C. Anastasiou, C. Duhr, F. Dulat and B. Mistlberger, *Soft triple-real radiation for Higgs production at N3LO*, *JHEP* **07** (2013) 003 [1302.4379].

[88] F. Brown, *On the decomposition of motivic multiple zeta values*, 1102.1310.

[89] O. Schnetz. Computer program HyperlogProcedures, https://www.math.fau.de/person/oliver-schnetz/.

[90] L. N. Lipatov, *Analytic properties of high energy production amplitudes in N=4 SUSY*, *Theor. Math. Phys.* **170** (2012) 166 [1008.1015].

[91] V. S. Fadin and L. N. Lipatov, *BFKL equation for the adjoint representation of the gauge group in the next-to-leading approximation at N=4 SUSY*, *Phys. Lett. B* **706** (2012) 470 [1111.0782].

[92] J. Bartels, L. N. Lipatov and A. Prygarin, *MHV amplitude for 3→3 gluon scattering in Regge limit*, *Phys. Lett. B* **705** (2011) 507 [1012.3178].

[93] L. J. Dixon, C. Duhr and J. Pennington, *Single-valued harmonic polylogarithms and the multi-Regge limit*, *JHEP* **10** (2012) 074 [1207.0186].

[94] J. Pennington, *The six-point remainder function to all loop orders in the multi-Regge limit*, *JHEP* **01** (2013) 059 [1209.5357].

[95] S. Caron-Huot, *When does the gluon reggeize?*, *JHEP* **05** (2015) 093 [1309.6521].

[96] G. P. Korchemsky, *On Near forward high-energy scattering in QCD*, *Phys. Lett. B* **325** (1994) 459 [hep-ph/9311294].

[97] I. A. Korchemskaya and G. P. Korchemsky, *High-energy scattering in QCD and cross singularities of Wilson loops*, *Nucl. Phys. B* **437** (1995) 127 [hep-ph/9409446].